



CERN-EP-2022-006
12 January 2022

First study of the two-body scattering involving charm hadrons

ALICE Collaboration*

Abstract

This article presents the first measurement of the interaction between charm hadrons and nucleons. The two-particle momentum correlations of pD^- and $\bar{p}D^+$ pairs are measured by the ALICE Collaboration in high-multiplicity pp collisions at $\sqrt{s} = 13$ TeV. The data are compatible with the Coulomb-only interaction hypothesis within $(1.1-1.5)\sigma$. The level of agreement slightly improves if an attractive nucleon(N) \bar{D} strong interaction is considered, in contrast to most model predictions which suggest an overall repulsive interaction. This measurement allows for the first time an estimation of the 68% confidence level interval for the isospin $I = 0$ inverse scattering length of the $N\bar{D}$ state $f_{0,I=0}^{-1} \in [-0.4, 0.9] \text{ fm}^{-1}$, assuming negligible interaction for the isospin $I = 1$ channel.

arXiv:2201.05352v2 [nucl-ex] 1 Dec 2022

© 2022 CERN for the benefit of the ALICE Collaboration.

Reproduction of this article or parts of it is allowed as specified in the CC-BY-4.0 license.

*See Appendix A for the list of collaboration members

1 Introduction

The study of the residual strong interaction among hadrons is a very active field within nuclear physics. This interaction can lead to the formation of bound states, such as nuclei, or molecular states as, for example, the $\Lambda(1405)$, which is considered as being generated from the attractive forces in the nucleon(N) \bar{K} - $\Sigma\pi$ channels [1–4]. One of the most fervent discussions in this context is nowadays revolving around systems involving charm mesons (D , D^*). Studies of their interaction are motivated by the observation of several new states with hidden charm and/or beauty (so-called XYZ states) [5–9], as well as with open charm such as the T_{cc}^+ [10, 11], and also of pentaquark states like $P_c(4380)$ and $P_c(4450)$ [12, 13]. These exotic hadrons can be described as compact multi-quark states in the context of the constituent-quark model [14], but are also considered as natural candidates for loosely bound molecular states [5, 6]. For example, the structure of the $\chi_{c1}(3872)$ (formerly $X(3872)$) has been interpreted as a $\bar{D}D^*/D\bar{D}^*$ molecular state or as a tetraquark [15]. Currently, definite conclusions are difficult to draw because of the lack of any direct experimental information on the $D\bar{D}^*$ strong interaction. Strong support for the molecular nature of the $\Lambda(1405)$ came not least from low-energy $N\bar{K}$ scattering data and information on the $p\bar{K}$ scattering length from kaonic hydrogen atoms [16–19]. Hence, a determination of the scattering parameters of systems involving D and/or D^* mesons are pivotal to advance in the interpretation of the many observed states. The first step in this direction is the investigation of the interaction between the $p(uud)D^-(\bar{c}d)$ pair and its charge conjugate. This interaction does not couple to the lower energy meson–baryon channels since no $q\bar{q}$ annihilation can occur. A measurement of this interaction is also an essential reference for the study of the in-medium D - and D^* -meson properties [20]. Similarly to kaons and antikaons, it is theoretically predicted that possible modifications of the charm-meson spectral function at large baryonic densities can be connected to a decrease of the chiral condensate, thus providing sensitivity to chiral-symmetry restoration [21].

So far, the topic of the strong interaction between hadrons containing charm quarks was addressed only from a theoretical point of view [22–25] by employing different effective models anchored to the successful description of other baryon–meson final states, such as the $N\bar{K}$ and NK systems, while data are missing. Scattering experiments [26] and systematic studies of stable and unstable nuclei [27], accompanied by sophisticated calculations achieved within effective field theories [28, 29], allowed us to reach a solid comprehension of the interaction among nucleons. When extending these studies to interactions including strange hadrons, the average properties of the interactions of some strange nucleon–hadron combinations (pK^\pm [30–32], $p\Lambda$, and $p\Sigma^0$ [33–35]) could be gauged with the help of scattering data and measurements of kaonic atoms [36]. The study of Λ hypernuclei [37] led to the extraction of an average attractive potential. The situation has drastically changed in recent years, thanks to the novel employment of the femtoscopy technique [38] in pp and p -Pb collisions at the LHC applied to almost all combinations of protons and strange hadrons [39]. The ALICE Collaboration could precisely study the following interactions: pp , pK^\pm , $p\Lambda$, $p\bar{\Lambda}$, $p\Sigma^0$, $\Lambda\Lambda$, $\Lambda\bar{\Lambda}$, $p\Xi^-$, $p\Omega^-$, and $p\phi$ [39–47]. Since conventional scattering experiments cannot be performed with D mesons and charm nuclei [48] have not been discovered yet (searches for charm nuclear states are included in the scientific program of the Japan Proton Accelerator Research Complex [49]), the femtoscopy technique can be employed to study the ND and $N\bar{D}$ interactions. In this article, the first measurement of the strong interaction between a D^- meson and a proton is reported. This pioneering analysis employs D^- instead of the more abundantly produced \bar{D}^0 mesons because of the smaller contribution from decays of excited charm states and the possibility to separate particles and antiparticles without ambiguity.

2 Experimental apparatus and data samples

The analysis was performed using a sample of high-multiplicity pp collisions at $\sqrt{s} = 13$ TeV collected by ALICE [50, 51] during the LHC Run 2 (2016–2018). The main detectors used for this analysis to reconstruct and identify the protons and the D -meson decay products are the Inner Tracking System

(ITS) [52], the Time Projection Chamber (TPC) [53] and the Time-Of-Flight (TOF) detector [54]. They are located inside a large solenoidal magnet providing a uniform magnetic field of 0.5 T parallel to the LHC beam direction and cover the pseudorapidity interval $|\eta| < 0.9$. The events were recorded with a high-multiplicity trigger relying on the measured signal amplitudes in the V0 detector, which consists of two scintillator arrays covering the pseudorapidity intervals $-3.7 < \eta < -1.7$ and $2.8 < \eta < 5.1$ [55]. The collected data sample corresponds to the 0.17% highest-multiplicity events out of all inelastic collisions with at least one charged particle in the pseudorapidity range $|\eta| < 1$ (denoted as INEL > 0). Events were further selected offline in order to remove machine-induced backgrounds [51]. The events were required to have a reconstructed collision vertex located within ± 10 cm from the center of the detector along the beam-line direction to maintain a uniform acceptance. Events with multiple primary vertices (pileup), reconstructed from track segments measured with the two innermost ITS layers, were rejected. The remaining undetected pileup is of the order of 1% and therefore negligible in the analysis. After these selections, the analyzed data sample consists of about 10^9 events. The Monte Carlo (MC) samples used in this analysis consist of pp collisions simulated using the PYTHIA 8.243 event generator [56, 57] with the Monash-13 tune [58] and GEANT3 [59] for the propagation of the generated particles through the detector.

3 Data analysis

3.1 Selection of proton and D^\pm -meson candidates

The proton candidates are selected according to the methods described in [39]. Charged-particle tracks reconstructed with the TPC are required to have transverse momentum $0.5 < p_T < 4.05$ GeV/ c and pseudorapidity $|\eta| < 0.8$. Particle identification (PID) is conducted by measuring the specific energy loss and the time of flight with the TPC and TOF detectors, respectively. The selection is based on the deviation n_σ between the measured and expected values for protons, normalized by the detector resolution σ . For proton candidates with a momentum $p < 0.75$ GeV/ c , only the TPC is used by requiring $|n_\sigma^{\text{TPC}}| < 3$, while for larger momenta the PID information of TPC and TOF are combined and tracks are accepted only if the condition $\sqrt{(n_\sigma^{\text{TPC}})^2 + (n_\sigma^{\text{TOF}})^2} < 3$ is fulfilled. With these selection criteria, the purity of the proton sample averaged over p_T is $P_p = 98\%$ [39]. The contribution of secondary protons originating from weak decays or interactions with the detector material is assessed by using MC template fits to the measured distribution of the distance of closest approach of the track to the primary vertex. The estimated average fraction of primary protons is 86% [39].

The D^\pm mesons are reconstructed via their hadronic decay channel $D^\pm \rightarrow K^\mp \pi^\pm \pi^\pm$, having a branching ratio $\text{BR} = (9.38 \pm 0.15)\%$ [60]. D-meson candidates are defined combining triplets of tracks reconstructed in the TPC and ITS detectors with the proper charge signs, $|\eta| < 0.8$, $p_T > 0.3$ GeV/ c , and a minimum of two (out of six) hits in the ITS, with at least one in either of the two innermost layers to ensure a good pointing resolution. To reduce the large combinatorial background and the contribution of D^\pm mesons originating from beauty-hadron decays (non-prompt), a machine-learning multi-class classification algorithm based on Boosted Decision Trees (BDT) provided by the XGBOOST library [61, 62] is employed. The variables utilized for the candidate selection in the BDT are based on the displaced decay-vertex topology, exploiting the mean proper decay length of D^\pm mesons of $c\tau \approx 312$ μm [60], and on the PID of charged pions and kaons. Before that, a preselection of the D^\pm candidates based on the PID information of the decay products is applied by requiring a 3σ compatibility either with the TPC or the TOF expected signals of the daughter tracks. Signal samples of prompt (originating from charm-quark hadronization or decays of excited charm states) and non-prompt D^\pm mesons for the BDT training are obtained from MC simulations. The background samples are obtained from the sidebands of the candidate invariant mass distributions in data. The BDT outputs are related to the candidate probability to be a prompt or non-prompt D meson, or combinatorial background. D-meson candidates are selected in the p_T interval between 1 and 10 GeV/ c by requiring a high probability to be a prompt D^\pm meson and a low

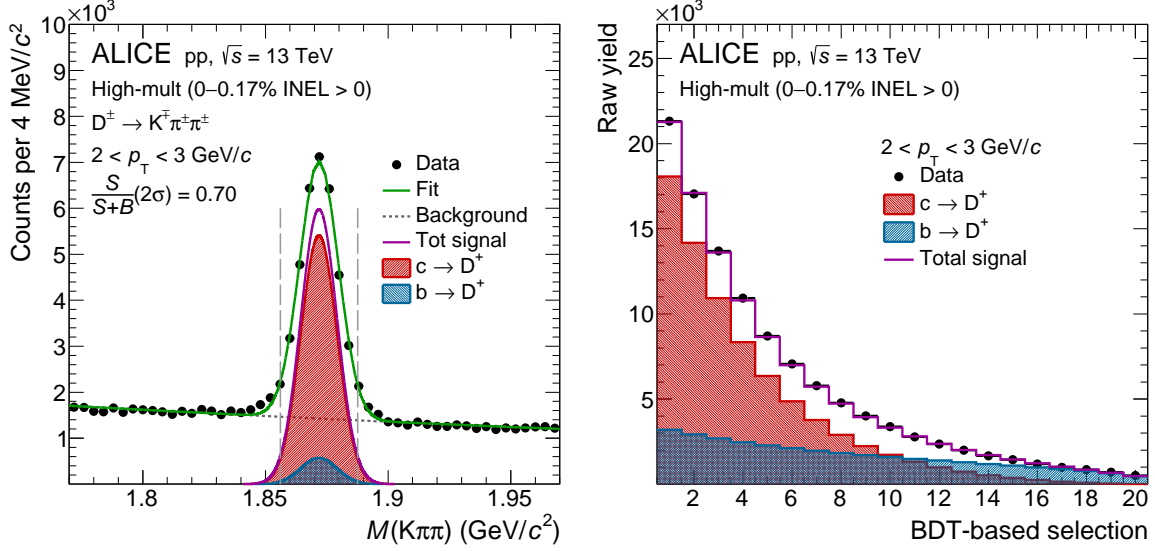


Figure 1: Left: invariant mass distributions of D^\pm candidates in the $2 < p_T < 3 \text{ GeV}/c$ interval. The green solid line shows the total fit function and the gray dotted line the combinatorial background. The contributions of D^\pm mesons originating from charm hadronisation and beauty-hadron decays are obtained with the method relying on the definition of different selection criteria, as explained in the text. Right: example of raw-yield distribution as a function of the BDT-based selection employed in the procedure adopted for the determination of the fraction of D^\pm originating from beauty-hadron decays for the $2 < p_T < 3 \text{ GeV}/c$ interval.

probability to be a combinatorial-background candidate.

A selection on the candidate invariant mass ($M(K\pi\pi)$) is applied to obtain a high-purity sample of D^\pm mesons. To this end, the $M(K\pi\pi)$ distribution of D^\pm candidates is fitted in intervals of p_T of 1 GeV width in the range $1 < p_T < 10 \text{ GeV}/c$ with a Gaussian function for the signal and an exponential term for the background. The left panel of Fig. 1 shows the $M(K\pi\pi)$ distribution for D^\pm with $2 < p_T < 3 \text{ GeV}/c$. The width of the Gaussian function used to describe the signal peak, σ_{D^\pm} , increases from 6 to 10 MeV/c^2 with increasing p_T as a consequence of the p_T dependence of the momentum resolution. The D^\pm -meson candidates in the invariant mass window $|M(K\pi\pi)| < 2\sigma_{D^\pm}$ are selected to be paired with proton candidates. This selection, displayed by the two vertical lines in Fig. 1, leads to a purity that is $P_{D^\pm} = (61.7 \pm 0.9(\text{stat}) \pm 0.7(\text{syst}))\%$ on average. The systematic uncertainty of P_{D^\pm} is evaluated by repeating the invariant mass fits, varying the background fit function and the invariant mass upper and lower limits.

The contributions of prompt and non-prompt D^\pm mesons are depicted in the left panel of Fig. 1 with the red and blue distributions, respectively. They are obtained with a data-driven method based on the sampling of the raw yield at different values of the BDT output score related to the probability of being a non-prompt D^\pm meson [63]. The yields of prompt and non-prompt D^\pm mesons can be extracted by solving a system of equations that relate the raw yield value Y_i (obtained with the i -th threshold on the BDT output score) to the corrected yields of prompt (N_{prompt}) and non-prompt ($N_{\text{non-prompt}}$) D^\pm mesons via the corresponding acceptance-times-efficiency factors for prompt ($(\text{Acc} \times \varepsilon)_i^{\text{prompt}}$) and non-prompt ($(\text{Acc} \times \varepsilon)_i^{\text{non-prompt}}$) D^\pm mesons as follows

$$\begin{pmatrix} (\text{Acc} \times \varepsilon)_1^{\text{prompt}} & (\text{Acc} \times \varepsilon)_1^{\text{non-prompt}} \\ \vdots & \vdots \\ (\text{Acc} \times \varepsilon)_n^{\text{prompt}} & (\text{Acc} \times \varepsilon)_n^{\text{non-prompt}} \end{pmatrix} \times \begin{pmatrix} N_{\text{prompt}} \\ N_{\text{non-prompt}} \end{pmatrix} - \begin{pmatrix} Y_1 \\ \vdots \\ Y_n \end{pmatrix} = \begin{pmatrix} \delta_1 \\ \vdots \\ \delta_n \end{pmatrix}. \quad (1)$$

The δ_i factors represent the residuals that account for the equations not holding exactly due to the

uncertainty of Y_i , $(\text{Acc} \times \varepsilon)_i^{\text{non-prompt}}$, and $(\text{Acc} \times \varepsilon)_i^{\text{prompt}}$. The system of equations can be solved via a χ^2 minimization, which leads to the determination of N_{prompt} and $N_{\text{non-prompt}}$. The right panel of Fig. 1 shows an example of a raw-yield distribution as a function of the BDT-based selection used in the minimization procedure for D^\pm mesons with $2 < p_T < 3$ GeV/ c . The leftmost data point of the distribution represents the raw yield corresponding to the loosest selection on the BDT output related to the candidate probability of being a non-prompt D^\pm meson, while the rightmost one corresponds to the strictest selection, which is expected to preferentially select non-prompt D^\pm mesons. The prompt and non-prompt components, obtained for each BDT-based selection using the procedure described above, are represented by the red and blue filled histograms, respectively, while their sum is reported by the magenta histogram.

The obtained corrected yields N_{prompt} and $N_{\text{non-prompt}}$ can then be used to compute the fraction of non-prompt D^\pm mesons $f_{\text{non-prompt}}^j$ for a given selection j ,

$$f_{\text{non-prompt}}^j = \frac{(\text{Acc} \times \varepsilon)_j^{\text{non-prompt}} \times N_{\text{non-prompt}}}{(\text{Acc} \times \varepsilon)_j^{\text{non-prompt}} \times N_{\text{non-prompt}} + (\text{Acc} \times \varepsilon)_j^{\text{prompt}} \times N_{\text{prompt}}}. \quad (2)$$

The $f_{\text{non-prompt}}$ factor for the selections used to build the pD^- and $\bar{p}D^+$ pairs is estimated to be $(7.7 \pm 0.5(\text{stat}) \pm 0.2(\text{syst}))\%$. The systematic uncertainty of $f_{\text{non-prompt}}$ is evaluated by repeating the procedure with different sets of selection criteria and varying the fitting parameters in the raw-yield extraction. In addition, since the efficiency depends on the charged-particle multiplicity, the multiplicity distribution in the MC sample used for the efficiency computation was weighted in order to reproduce the one in data.

Differently from the component originating from beauty-hadron weak decays, D^\pm mesons originating from excited charm-meson strong decays cannot be experimentally resolved from promptly produced D^\pm mesons due to their short lifetime. The two largest sources are the $D^{*\pm} \rightarrow D^\pm \pi^0$ and $D^{*\pm} \rightarrow D^\pm \gamma$ decays, having $\text{BR} = (30.7 \pm 0.5)\%$ and $\text{BR} = (1.6 \pm 0.4)\%$ [60], respectively. Their contribution is estimated from the production cross sections of D^+ and D^{*+} mesons measured in pp collisions at $\sqrt{s} = 5.02$ TeV [63, 64] and employing the PYTHIA 8 decayer for the description of the $D^{*\pm} \rightarrow D^\pm X$ decay kinematics. The fraction of D^\pm mesons in $1 < p_T < 10$ GeV/ c originating from $D^{*\pm}$ decays is estimated to be $f_{D^{*\pm}} = (27.6 \pm 1.3(\text{stat}) \pm 2.4(\text{syst}))\%$, where statistical and systematic uncertainties are propagated from the measurements of the D^+ and D^{*+} production cross sections.

3.2 The correlation function

The proton and D^- candidates are then combined and their relative momentum k^* is evaluated as $k^* = \frac{1}{2} \times |\mathbf{p}_p^* - \mathbf{p}_D^*|$, where $\mathbf{p}_{p,D}^*$ are the momenta of the two particles in the pair rest frame. The k^* distribution of pD^- pairs, $N_{\text{same}}(k^*)$, is then divided by the one obtained combining proton and D^- candidates from different events, $N_{\text{mixed}}(k^*)$, to compute the two-particle momentum correlation function, which is defined as $C_{\text{exp}}(k^*) = \mathcal{N} \times N_{\text{same}}(k^*)/N_{\text{mixed}}(k^*)$ [65]. The latter provides a correction for the acceptance of the detector and the normalization for the phase space of the particle pairs. To ensure the same geometrical acceptance as for N_{same} , the mixing procedure is conducted only between particle pairs produced in events with similar z position of the primary vertex and similar charged-particle multiplicity. Since the correlation functions for pD^- and $\bar{p}D^+$ are consistent with each other within statistical uncertainties, they are combined and in the following pD^- will represent $pD^- \oplus \bar{p}D^+$. The normalization constant \mathcal{N} is obtained from $k^* \in [1500, 2000]$ MeV/ c where the correlation function is independent of k^* , as expected since in this region of k^* the pairs of particles are not affected by any interaction. The resulting correlation function $C_{\text{exp}}(k^*)$ is displayed in the left panel of Fig. 2. The data are compatible with unity for $k^* > 500$ MeV/ c , while they show a possible hint of an increase for lower k^* values. In total 200 pD^- and 221 $\bar{p}D^+$ pairs contribute to $N_{\text{same}}(k^*)$ in the region of $k^* < 200$ MeV/ c , where model calculations [22–25] predict a deviation from unity. The systematic

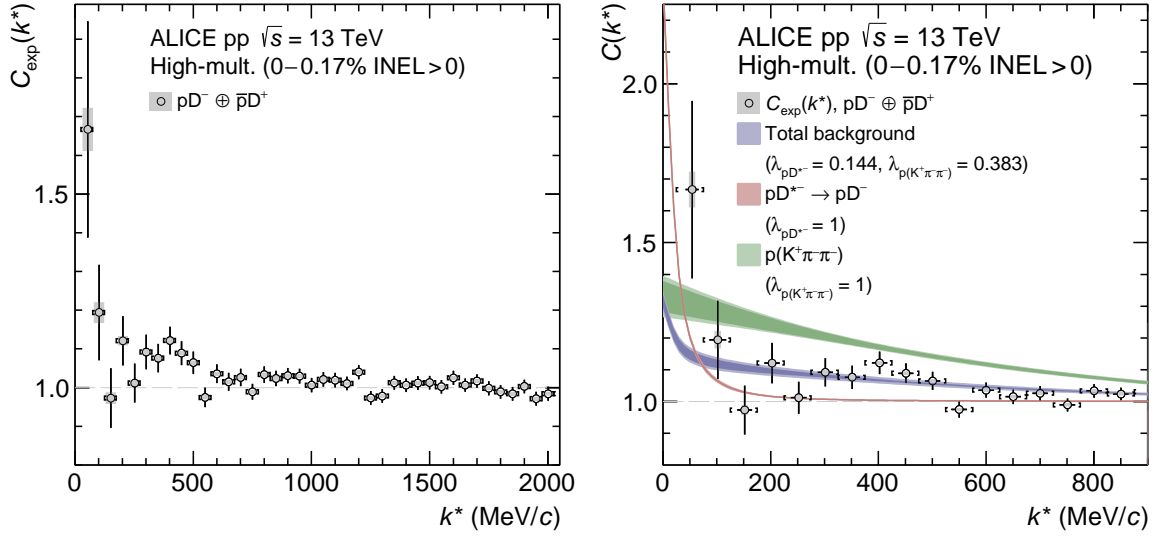


Figure 2: Left: experimental pD^- correlation function in the range $0 < k^* < 2$ GeV/c. Statistical (bars) and systematic uncertainties (shaded boxes) are shown separately. The open boxes represent the bin width. Right: experimental pD^- correlation function in a reduced k^* range together with the contributions from $p(K^+\pi^-\pi^-)$ (green band) and pD^{*-} (red band), and the total background model (purple band). The $p(K^+\pi^-\pi^-)$ and pD^{*-} contributions are not scaled by the respective λ parameter. The width of the dark (light) shaded bands depicts the statistical (total) uncertainty of the parametrized background contributions.

uncertainties of $C_{\text{exp}}(k^*)$ are assessed by varying the proton and D^- selection criteria.

The measured two-particle momentum correlation function can be related to the source function and the two-particle wave function via the Koonin–Pratt equation $C(k^*) = \int d^3r^* S(r^*) |\Psi(k^*, r^*)|^2$ [65], where $S(r^*)$ is the source function, $\Psi(k^*, r^*)$ is the two-particle wave function, and r^* refers to the relative distance between the two particles. The source function for the pD^- pairs is estimated by employing the hypothesis of a common source for all hadrons in high-multiplicity pp collisions at the LHC corrected for strong decays of extremely short-lived resonances ($c\tau \lesssim 5$ fm) feeding into the particle pairs [66]. This is the case for resonances strongly decaying into protons. In contrast, both beauty-hadron and $D^{*\pm}$ decays occur at larger distances than the typical range for the strong interaction [60]. This implies that the correlation function for D^- mesons originating from these decays will only carry the imprint of the interaction of the parent particle with the proton without impacting the size of the emitting source. The core source determined in [66] features a dependence on the transverse mass m_T of the particle pair, which can be attributed to a collective expansion of the system [65, 67–69]. The collective behavior has been studied in high-multiplicity pp collisions by the CMS Collaboration and found to be comparable for light-flavor and charm hadrons [70]. Hence, the core source of pD^- pairs with $k^* < 200$ MeV/c is estimated by parameterizing the measured m_T dependence of the source radius extracted from pp correlations in [66] and evaluating it at the $\langle m_T \rangle = 2.7$ GeV/ c^2 of the pD^- pairs. Since the production mechanism of charm mesons might not be identical to that of light-flavor baryons, the emission of the pp and pD^- pairs is studied by simulating pp collisions with PYTHIA 8.301 [57] and computing their relative distance in the pair rest frame, r^* , considering only D^- mesons originating directly from charm-quark hadronization. These studies indicate that the core source of pD^- at the pertinent $\langle m_T \rangle$ is smaller by about 25% compared to that of pp pairs. This is included in the systematic uncertainty of the source radius. The resulting overall source is parametrized by a Gaussian profile characterized by an effective radius $R_{\text{eff}} = 0.89^{+0.08}_{-0.22}$ fm, where the uncertainty includes both the one arising from the m_T -dependent parametrization and the PYTHIA 8 study.

The correlation function due to the genuine pD^- interaction can be extracted from the measured $C_{\text{exp}}(k^*)$

by estimating and subtracting the contributions of D^- mesons originating from beauty-hadron and D^{*-} decays, protons originating from strange-hadron decays, as well as misidentified protons and combinatorial-background D -meson candidates. The experimental correlation function is decomposed as

$$C_{\text{exp}}(k^*) = \lambda_{\text{pD}^-} \times C_{\text{pD}^-}(k^*) + \lambda_{\text{p(K}^+\pi^-\pi^-)} \times C_{\text{p(K}^+\pi^-\pi^-)}(k^*) + \lambda_{\text{pD}^{*-}} \times C_{\text{pD}^{*-}}(k^*) + \lambda_{\text{flat}} \times C_{\text{flat}}. \quad (3)$$

The combinatorial ($\text{K}^+\pi^-\pi^-$) background below the D^- peak and the final-state interaction among protons and D^- from D^{*-} decays play a significant role. All other contributions are assumed to be characterized by a $C(k^*)$ compatible with unity and are therefore included in the C_{flat} contribution. The relative weights, λ_i , are evaluated considering the contributions to D^- candidates described above and following the procedure explained in [39] for the protons. They are about 33.9% for $C_{\text{pD}^-}(k^*)$ and 38.8%, 14.4%, and 13.4% for the $\text{p(K}^+\pi^-\pi^-)$, pD^{*-} , and flat contributions, respectively.

The correlation function $C_{\text{p(K}^+\pi^-\pi^-)}$ is extracted from the sidebands of the D^- candidates, chosen as $[M_{\text{D}^-}(p_{\text{T}}) - 200 \text{ MeV}/c, M_{\text{D}^-}(p_{\text{T}}) - 5 \times \sigma_{\text{D}^-}(p_{\text{T}})]$ and $[M_{\text{D}^-}(p_{\text{T}}) + 5 \times \sigma_{\text{D}^-}(p_{\text{T}}), M_{\text{D}^-}(p_{\text{T}}) + 200 \text{ MeV}/c]$ for the left and right sidebands, respectively. The contamination from $D^{*-} \rightarrow \bar{\text{D}}^0 \pi^- \rightarrow \text{K}^+ \pi^- \pi^-$ decays in the right sideband is suppressed by a $2.5\sigma_{\text{D}^{*-}}$ rejection around the mean value of the D^{*-} invariant mass peak. The resulting correlation function is parametrized by a third-order polynomial in $k^* \in [0, 1.5] \text{ GeV}/c$ and is displayed by the green curve reported in the right panel of Fig. 2. The observed behavior is determined by meson–meson and baryon–meson mini-jets and residual two-body interactions among the quadruplet, as obtained from previous studies [42, 46].

The residual pD^{*-} correlation function is computed employing the Koonin–Pratt formalism using the CATS framework [71] to obtain a two-particle wave function $\Psi(k^*, r^*)$ considering only the Coulomb interaction and assuming that the source radius is the same as for pD^- pairs. The obtained pD^{*-} correlation function is transformed to the momentum basis of the pD^- relative momentum by considering the kinematics of the $D^{*-} \rightarrow \text{D}^- \text{X}$ decay [72]. The resulting correlation function is shown in the right panel of Fig. 2 as a red band. The purple band in the same figure represents the total background that includes all contributions with their corresponding weights. Finally, the genuine pD^- correlation function is obtained by solving Eq. 3 for $C_{\text{pD}^-}(k^*)$ and is shown in Fig. 3.

The systematic uncertainties of the genuine pD^- correlation function, $C_{\text{pD}^-}(k^*)$, include (i) the uncertainties of $C_{\text{exp}}(k^*)$, (ii) the uncertainties of the λ_i weights, and (iii) the uncertainties related to the parametrization of the background sources, $C_{\text{p(K}^+\pi^-\pi^-)}(k^*)$ and $C_{\text{pD}^{*-}}(k^*)$. In particular, as previously mentioned, the systematic uncertainty on $C_{\text{exp}}(k^*)$ is estimated by varying the proton and D^- -candidate selection criteria and ranges between 0.5% and 3% as a function of k^* . The uncertainties of the λ_i weights are derived from the systematic uncertainties on the proton and D^- purities (P_{p} and P_{D^-}), $f_{\text{D}^{*-}}$, and $f_{\text{non-prompt}}$ reported in Section 3.1. The systematic uncertainties of $C_{\text{p(K}^+\pi^-\pi^-)}(k^*)$ are estimated following the same procedure adopted for $C_{\text{exp}}(k^*)$ and, in addition, by varying the range of the fit of the correlation function parametrized from the sidebands regions of the invariant mass distribution. Additional checks are performed by varying the invariant mass interval used to define the sidebands region of up to $100 \text{ MeV}/c^2$. The resulting systematic uncertainty ranges from 1% to 5%. The systematic uncertainty of $C_{\text{pD}^{*-}}(k^*)$ is due to the uncertainty on the emitting source. Considering the small $\lambda_{\text{pD}^{*-}}(k^*)$ this uncertainty results to be negligible compared to the other sources of uncertainty. The overall relative systematic uncertainty on $C_{\text{pD}^-}(k^*)$ resulting from the different sources ranges between 3% and 10% and is maximum in the lowest k^* interval.

4 Results

The resulting genuine $C_{\text{pD}^-}(k^*)$ correlation function can be employed to study the pD^- strong interaction that is characterized by two isospin configurations and is coupled to the $\bar{\text{nD}}^0$ channel. First of all, in order

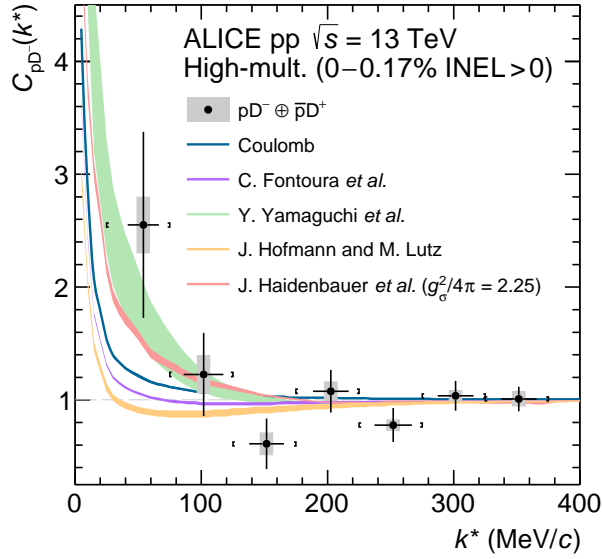


Figure 3: Genuine pD^- correlation function compared with different theoretical models (see text for details). The null hypothesis is represented by the curve corresponding to the Coulomb interaction only.

to assess the effect of the strong interaction on the correlation function, a reference calculation including only the Coulomb interaction is considered. The corresponding correlation function is obtained using CATS [71]. Secondly, various theoretical approaches to describe the strong interaction are benchmarked, including meson exchange (J. Haidenbauer et al. [22]), meson exchange based on heavy quark symmetry (Y. Yamaguchi et al. [25]), an SU(4) contact interaction (J. Hoffmann and M. Lutz [23]), and a chiral quark model (C. Fontoura et al. [24]). The relative wave functions for the model of J. Haidenbauer et al. [22] are provided directly, while for the other models [23–25] they are evaluated by employing a Gaussian potential whose strength is adjusted to describe the corresponding published $I = 0$ and $I = 1$ scattering lengths listed in Table 1. The pD^- correlation function is computed within the Koonin–Pratt formalism, taking into account explicitly the coupling between the pD^- and $n\bar{D}^0$ channels [73] and including the Coulomb interaction [74]. The finite experimental momentum resolution is considered in the modeling of the correlation functions [39].

The outcome of these models is compared in Fig. 3 with the measured genuine pD^- correlation function. The degree of consistency between data and models is quantified by the p-value computed in the range $k^* < 200$ MeV/c. It is expressed by the number of standard deviations n_σ reported in Table 1, where the n_σ range accounts, at one standard deviation level, for the total uncertainties of the data points and the models. The values of the scattering lengths f_0 for the different models are also reported in Table 1. Here, the high-energy physics convention on the scattering-length sign is adopted: a negative value corresponds to either a repulsive interaction or to an attractive one with presence of a bound state, while a positive value corresponds to an attractive interaction. The data are compatible with the Coulomb-only hypothesis within $(1.1\text{--}1.5)\sigma$. Nevertheless, the level of agreement slightly improves in case of the models by J. Haidenbauer et al. (employing $g_\sigma^2/4\pi = 2.25$) which predicts an attractive interaction, and by Y. Yamaguchi et al. which foresees the formation of a $N\bar{D}$ bound state with a mass of 2804 MeV/c² in the $I = 0$ channel.

Finally, the scattering parameters can be constrained by comparing the data with the outcome of calculations carried out varying the strength of the potential and the source radius. In this case the interaction potential is parametrized by a Gaussian-type functional form with the range of ρ -meson exchange. In this estimation, it is assumed that the interaction in the $I = 1$ channel is negligible for simplicity. The correlation function $C_{pD^-}(k^*)$ is computed including also the Coulomb interaction and the coupled channel.

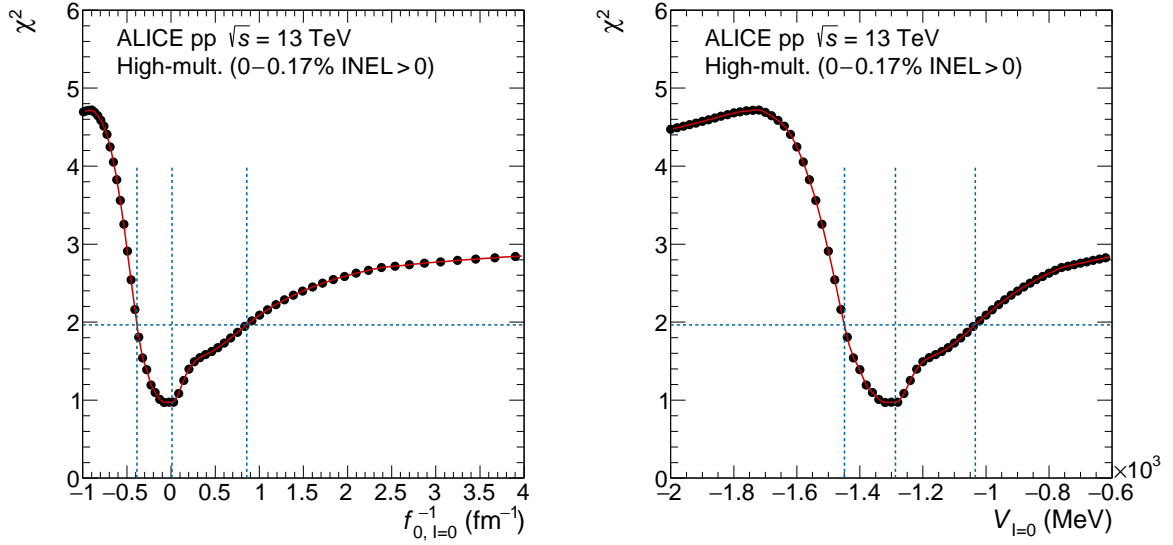


Figure 4: χ^2 distributions obtained by comparing the measured $C_{pD^-}(k^*)$ for $k^* < 200$ MeV/ c with the correlation function calculated with an interaction modeled by a Gaussian potential with an interaction range given by ρ -meson exchanges as a function of the inverse scattering length (left panel) and the interaction potential (right panel) for $I = 0$. The blue dotted lines represent the value of $f_{0,I=0}^{-1}$ and $V_{I=0} = 0$ for which the χ^2 is minimum and for the 1σ confidence interval.

This procedure is repeated for different values of the interaction potential for the $I = 0$ channel ($V_{I=0}$). For all the correlation functions corresponding to the different interaction potentials, the agreement with the data is evaluated by computing the χ^2 using a bootstrap procedure. Both the statistical and systematic uncertainties of the data are considered in the bootstrap procedure, as well as the uncertainty on the emitting source radius (R_{eff}) in the computed $C_{pD^-}(k^*)$, which is varied within 1σ of its uncertainty. The resulting overall χ^2 distributions are shown in Fig. 4 as a function of $f_{0,I=0}^{-1}$ and $V_{I=0}$ in the left and right panels, respectively. The data are found to be consistent with a potential strength of $V_{I=0} \in [-1450, -1050]$ MeV within 1σ . This corresponds to an inverse scattering-length interval of $f_{0,I=0}^{-1} \in [-0.4, 0.9]$ fm $^{-1}$. Since the determined potential strength is always attractive, the positive values of the scattering length imply an attractive interaction without bound states, while the negative values are consistent with the presence of a $N\bar{D}$ bound state. The same procedure was repeated for fixed values of R_{eff} in order to obtain the 1σ confidence interval as a function of the emitting source radius. Figure 5 shows the confidence interval as a function of the source radius varied within 1σ of its uncertainty. The dashed interval corresponds to the radius uncertainty due to only the m_T dependence while the full-shaded interval shows the total radius uncertainty. The most probable value reported in Fig 5 with the star symbol corresponds to an attractive interaction with the formation of a bound state. Given that most models predict a repulsive $I = 1$ interaction, in reality the $I = 0$ interaction might have to be even more attractive. The herewith presented limits provide valuable guidance for further theoretical studies advancing the understanding of

Table 1: Scattering parameters of the different theoretical models for the $N\bar{D}$ interaction [22–25] and degree of consistency with the experimental data computed in the range $k^* < 200$ MeV/ c .

Model	$f_0(I=0)$	$f_0(I=1)$	n_σ
Coulomb			(1.1–1.5)
Haidenbauer et al. [22] ($g_\sigma^2/4\pi = 2.25$)	0.67	0.04	(0.8–1.3)
Hofmann and Lutz [23]	−0.16	−0.26	(1.3–1.6)
Yamaguchi et al. [25]	−4.38	−0.07	(0.6–1.1)
Fontoura et al. [24]	0.16	−0.25	(1.1–1.5)

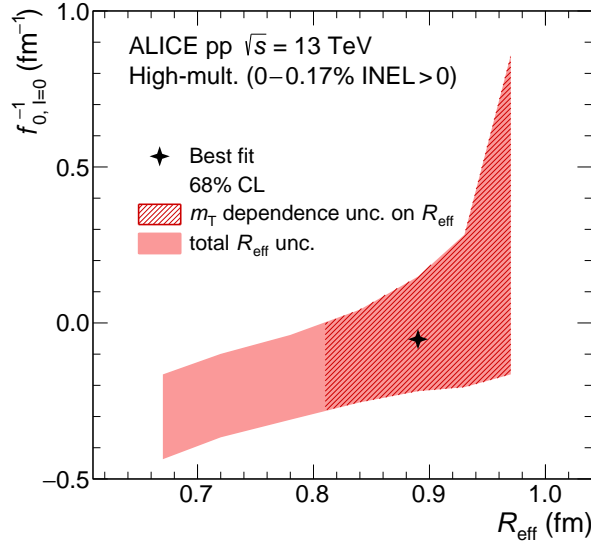


Figure 5: Regions of 68% confidence intervals for the inverse scattering length $f_{0,I=0}^{-1}$ as a function of the source radius varied within one standard deviation considering only the m_T dependence on R_{eff} and the total uncertainty (see text for details) under the assumption of negligible interaction for $I = 1$. The most probable value is reported by the star symbol.

the strong interaction in the charm sector.

5 Summary

In conclusion, this article presents the first measurement of correlation functions involving charm hadrons, which allows one to access to the strong interaction between a proton and a charm meson. The genuine pD^- correlation function reflects the pattern of an overall attractive interaction. The data are compatible within $(1.1-1.5)\sigma$ with the correlation function obtained from the hypothesis of a Coulomb-only interaction. The degree of consistency improves when considering, in addition, state-of-the-art models that predict an attractive strong $N\bar{D}$ interaction with or without a bound state. Finally, assuming no interaction for the $I = 1$ channel, the scattering length of the $N\bar{D}$ system in the isospin $I = 0$ channel is estimated as $f_{0,I=0}^{-1} \in [-0.4, 0.9] \text{ fm}^{-1}$. This exploratory study paves the way for precision studies of the strong interactions involving charm hadrons, facilitated by about one order of magnitude larger pp data samples expected to be collected in the next years during the LHC Runs 3 and 4 [75].

Acknowledgements

The ALICE Collaboration would like to thank all its engineers and technicians for their invaluable contributions to the construction of the experiment and the CERN accelerator teams for the outstanding performance of the LHC complex. The ALICE Collaboration gratefully acknowledges the resources and support provided by all Grid centres and the Worldwide LHC Computing Grid (WLCG) collaboration. The ALICE Collaboration acknowledges the following funding agencies for their support in building and running the ALICE detector: A. I. Alkhanyan National Science Laboratory (Yerevan Physics Institute) Foundation (ANSL), State Committee of Science and World Federation of Scientists (WFS), Armenia; Austrian Academy of Sciences, Austrian Science Fund (FWF): [M 2467-N36] and Nationalstiftung für Forschung, Technologie und Entwicklung, Austria; Ministry of Communications and High Technologies, National Nuclear Research Center, Azerbaijan; Conselho Nacional de Desenvolvimento Científico e Tecnológico (CNPq), Financiadora de Estudos e Projetos (Finep), Fundação de Amparo à

Pesquisa do Estado de São Paulo (FAPESP) and Universidade Federal do Rio Grande do Sul (UFRGS), Brazil; Ministry of Education of China (MOEC), Ministry of Science & Technology of China (MSTC) and National Natural Science Foundation of China (NSFC), China; Ministry of Science and Education and Croatian Science Foundation, Croatia; Centro de Aplicaciones Tecnológicas y Desarrollo Nuclear (CEADEN), Cubaenergía, Cuba; Ministry of Education, Youth and Sports of the Czech Republic, Czech Republic; The Danish Council for Independent Research | Natural Sciences, the VILLUM FONDEN and Danish National Research Foundation (DNRF), Denmark; Helsinki Institute of Physics (HIP), Finland; Commissariat à l’Energie Atomique (CEA) and Institut National de Physique Nucléaire et de Physique des Particules (IN2P3) and Centre National de la Recherche Scientifique (CNRS), France; Bundesministerium für Bildung und Forschung (BMBF) and GSI Helmholtzzentrum für Schwerionenforschung GmbH, Germany; General Secretariat for Research and Technology, Ministry of Education, Research and Religions, Greece; National Research, Development and Innovation Office, Hungary; Department of Atomic Energy Government of India (DAE), Department of Science and Technology, Government of India (DST), University Grants Commission, Government of India (UGC) and Council of Scientific and Industrial Research (CSIR), India; Indonesian Institute of Science, Indonesia; Istituto Nazionale di Fisica Nucleare (INFN), Italy; Japanese Ministry of Education, Culture, Sports, Science and Technology (MEXT) and Japan Society for the Promotion of Science (JSPS) KAKENHI, Japan; Consejo Nacional de Ciencia (CONACYT) y Tecnología, through Fondo de Cooperación Internacional en Ciencia y Tecnología (FONCICYT) and Dirección General de Asuntos del Personal Académico (DGAPA), Mexico; Nederlandse Organisatie voor Wetenschappelijk Onderzoek (NWO), Netherlands; The Research Council of Norway, Norway; Commission on Science and Technology for Sustainable Development in the South (COMSATS), Pakistan; Pontificia Universidad Católica del Perú, Peru; Ministry of Education and Science, National Science Centre and WUT ID-UB, Poland; Korea Institute of Science and Technology Information and National Research Foundation of Korea (NRF), Republic of Korea; Ministry of Education and Scientific Research, Institute of Atomic Physics, Ministry of Research and Innovation and Institute of Atomic Physics and University Politehnica of Bucharest, Romania; Joint Institute for Nuclear Research (JINR), Ministry of Education and Science of the Russian Federation, National Research Centre Kurchatov Institute, Russian Science Foundation and Russian Foundation for Basic Research, Russia; Ministry of Education, Science, Research and Sport of the Slovak Republic, Slovakia; National Research Foundation of South Africa, South Africa; Swedish Research Council (VR) and Knut & Alice Wallenberg Foundation (KAW), Sweden; European Organization for Nuclear Research, Switzerland; Suranaree University of Technology (SUT), National Science and Technology Development Agency (NSDTA), Suranaree University of Technology (SUT), Thailand Science Research and Innovation (TSRI) and National Science, Research and Innovation Fund (NSRF), Thailand; Turkish Energy, Nuclear and Mineral Research Agency (TENMAK), Turkey; National Academy of Sciences of Ukraine, Ukraine; Science and Technology Facilities Council (STFC), United Kingdom; National Science Foundation of the United States of America (NSF) and United States Department of Energy, Office of Nuclear Physics (DOE NP), United States of America.

References

- [1] T. Hyodo and D. Jido, “The nature of the $\Lambda(1405)$ resonance in chiral dynamics”, *Prog. Part. Nucl. Phys.* **67** (2012) 55–98, arXiv:1104.4474 [nucl-th].
- [2] U.-G. Meißner, “Two-pole structures in QCD: Facts, not fantasy!”, *Symmetry* **12** (2020) 981, arXiv:2005.06909 [hep-ph].
- [3] M. Mai, “Review of the $\Lambda(1405)$ A curious case of a strangeness resonance”, *Eur. Phys. J. ST* **230** (2021) 1593–1607, arXiv:2010.00056 [nucl-th].

- [4] T. Hyodo and M. Niiyama, “QCD and the strange baryon spectrum”, *Prog. Part. Nucl. Phys.* **120** (2021) 103868, arXiv:2010.07592 [hep-ph].
- [5] E. S. Swanson, “The New heavy mesons: A Status report”, *Phys. Rept.* **429** (2006) 243–305, arXiv:hep-ph/0601110.
- [6] F.-K. Guo, C. Hanhart, U.-G. Meißner, Q. Wang, Q. Zhao, and B.-S. Zou, “Hadronic molecules”, *Rev. Mod. Phys.* **90** (2018) 015004, arXiv:1705.00141 [hep-ph].
- [7] A. Hosaka, T. Iijima, K. Miyabayashi, Y. Sakai, and S. Yasui, “Exotic hadrons with heavy flavors: X, Y, Z, and related states”, *PTEP* **2016** (2016) 062C01, arXiv:1603.09229 [hep-ph].
- [8] N. Brambilla, S. Eidelman, C. Hanhart, A. Nefediev, C.-P. Shen, C. E. Thomas, A. Vairo, and C.-Z. Yuan, “The XYZ states: experimental and theoretical status and perspectives”, *Phys. Rept.* **873** (2020) 1–154, arXiv:1907.07583 [hep-ex].
- [9] **LHCb** Collaboration, R. Aaij *et al.*, “Near-threshold $D\bar{D}$ spectroscopy and observation of a new charmonium state”, *JHEP* **07** (2019) 035, arXiv:1903.12240 [hep-ex].
- [10] **LHCb** Collaboration, R. Aaij *et al.*, “Observation of an exotic narrow doubly charmed tetraquark”, *Nature Phys.* **18** (2022) 751–754, arXiv:2109.01038 [hep-ex].
- [11] **LHCb** Collaboration, R. Aaij *et al.*, “Study of the doubly charmed tetraquark T_{cc}^{++} ”, *Nature Commun.* **13** (2022) 3351, arXiv:2109.01056 [hep-ex].
- [12] **LHCb** Collaboration, R. Aaij *et al.*, “Observation of $J/\psi p$ Resonances Consistent with Pentaquark States in $\Lambda_b^0 \rightarrow J/\psi K^- p$ Decays”, *Phys. Rev. Lett.* **115** (2015) 072001, arXiv:1507.03414 [hep-ex].
- [13] **LHCb** Collaboration, R. Aaij *et al.*, “Observation of a narrow pentaquark state, $P_c(4312)^+$, and of two-peak structure of the $P_c(4450)^+$ ”, *Phys. Rev. Lett.* **122** (2019) 222001, arXiv:1904.03947 [hep-ex].
- [14] M. Gell-Mann, “A Schematic Model of Baryons and Mesons”, *Phys. Lett.* **8** (1964) 214–215.
- [15] H.-X. Chen, W. Chen, X. Liu, and S.-L. Zhu, “The hidden-charm pentaquark and tetraquark states”, *Phys. Rept.* **639** (2016) 1–121, arXiv:1601.02092 [hep-ph].
- [16] B. Borasoy, R. Nissler, and W. Weise, “Kaonic hydrogen and K- p scattering”, *Phys. Rev. Lett.* **94** (2005) 213401, arXiv:hep-ph/0410305.
- [17] **SIDDHARTA** Collaboration, M. Bazzi *et al.*, “A New Measurement of Kaonic Hydrogen X-rays”, *Phys. Lett. B* **704** (2011) 113–117, arXiv:1105.3090 [nucl-ex].
- [18] Y. Ikeda, T. Hyodo, and W. Weise, “Improved constraints on chiral SU(3) dynamics from kaonic hydrogen”, *Phys. Lett. B* **706** (2011) 63–67, arXiv:1109.3005 [nucl-th].
- [19] Y. Ikeda, T. Hyodo, and W. Weise, “Chiral SU(3) theory of antikaon-nucleon interactions with improved threshold constraints”, *Nucl. Phys. A* **881** (2012) 98–114, arXiv:1201.6549 [nucl-th].
- [20] M. He, R. J. Fries, and R. Rapp, “Thermal Relaxation of Charm in Hadronic Matter”, *Phys. Lett. B* **701** (2011) 445–450, arXiv:1103.6279 [nucl-th].
- [21] L. Tolós, C. García-Recio, and J. Nieves, “The Properties of D and D* mesons in the nuclear medium”, *Phys. Rev. C* **80** (2009) 065202, arXiv:0905.4859 [nucl-th].

- [22] J. Haidenbauer, G. Krein, U.-G. Meißner, and A. Sibirtsev, “ $\bar{D}N$ interaction from meson-exchange and quark-gluon dynamics”, *Eur. Phys. J. A* **33** (2007) 107–117, arXiv:0704.3668 [nucl-th].
- [23] J. Hofmann and M. F. M. Lutz, “Coupled-channel study of crypto-exotic baryons with charm”, *Nucl. Phys. A* **763** (2005) 90–139, arXiv:hep-ph/0507071.
- [24] C. E. Fontoura, G. Krein, and V. E. Vizcarra, “ $\bar{D}N$ interaction in a color-confining chiral quark model”, *Phys. Rev. C* **87** (2013) 025206, arXiv:1208.4058 [nucl-th].
- [25] Y. Yamaguchi, S. Ohkoda, S. Yasui, and A. Hosaka, “Exotic baryons from a heavy meson and a nucleon – Negative parity states –”, *Phys. Rev. D* **84** (2011) 014032, arXiv:1105.0734 [hep-ph].
- [26] Stoks, Klomp, Rentmeester, and J. deSwaart, “Partial-wave analysis of all nucleon-nucleon scattering data below 350 mev.”, *Physical review. C, Nuclear physics* **48 2** (1993) 792–815.
- [27] F. Nowacki, A. Obertelli, and A. Poves, “The neutron-rich edge of the nuclear landscape: Experiment and theory.”, *Prog. Part. Nucl. Phys.* **120** (2021) 103866, arXiv:2104.06238 [nucl-th].
- [28] K. Hebeler, J. D. Holt, J. Menendez, and A. Schwenk, “Nuclear forces and their impact on neutron-rich nuclei and neutron-rich matter”, *Ann. Rev. Nucl. Part. Sci.* **65** (2015) 457–484, arXiv:1508.06893 [nucl-th].
- [29] E. Gebrerufael, K. Vobig, H. Hergert, and R. Roth, “Ab Initio Description of Open-Shell Nuclei: Merging No-Core Shell Model and In-Medium Similarity Renormalization Group”, *Phys. Rev. Lett.* **118** (2017) 152503, arXiv:1610.05254 [nucl-th].
- [30] G. S. Abrams and B. Sechi-Zorn, “Charge-Exchange Scattering of Low-Energy K- Mesons in Hydrogen”, *Phys. Rev.* **139** (1965) B454–B457.
- [31] J. S. Hyslop, R. A. Arndt, L. D. Roper, and R. L. Workman, “Partial wave analysis of K^+ nucleon scattering”, *Phys. Rev.* **D46** (1992) 961–969.
- [32] A. Olin and T. S. Park, “Kaon nucleon scattering and reactions at low energies”, *Nucl. Phys.* **A691** (2001) 295–303.
- [33] F. Eisele, H. Filthuth, W. Foehlich, V. Hepp, and G. Zech, “Elastic $\Sigma^\pm p$ scattering at low energies”, *Phys. Lett. B* **37** (1971) 204–206.
- [34] G. Alexander, U. Karshon, A. Shapira, G. Yekutieli, R. Engelmann, H. Filthuth, and W. Lughofer, “Study of the $\Lambda-N$ system in low-energy $\Lambda-p$ elastic scattering”, *Phys. Rev.* **173** (1968) 1452–1460.
- [35] B. Sechi-Zorn, B. Kehoe, J. Twitty, and R. Burnstein, “Low-energy Λ -proton elastic scattering”, *Phys. Rev.* **175** (1968) 1735–1740.
- [36] J. Hrtánková and J. Mareš, “ K^- - nuclear states: Binding energies and widths”, *Phys. Rev. C* **96** (2017) 015205, arXiv:1704.07205 [nucl-th].
- [37] A. Feliciello and T. Nagae, “Experimental review of hypernuclear physics: recent achievements and future perspectives”, *Rept. Prog. Phys.* **78** (2015) 096301.
- [38] S. Pratt, “Pion Interferometry of Quark-Gluon Plasma”, *Phys. Rev. D* **33** (1986) 1314–1327.
- [39] ALICE Collaboration, S. Acharya *et al.*, “p-p, p- Λ and Λ - Λ correlations studied via femtoscopy in pp reactions at $\sqrt{s} = 7$ TeV”, *Phys. Rev. C* **99** (2019) 024001, arXiv:1805.12455 [nucl-ex].

- [40] ALICE Collaboration, S. Acharya *et al.*, “Scattering studies with low-energy kaon-proton femtoscopy in proton-proton collisions at the LHC”, *Phys. Rev. Lett.* **124** (2020) 092301, arXiv:1905.13470 [nucl-ex].
- [41] ALICE Collaboration, S. Acharya *et al.*, “Exploring the $N\Lambda$ – $N\Sigma$ coupled system with high precision correlation techniques at the LHC”, *Phys. Lett. B* **833** (2022) 137272, arXiv:2104.04427 [nucl-ex].
- [42] ALICE Collaboration, S. Acharya *et al.*, “Investigation of the p – Σ^0 interaction via femtoscopy in pp collisions”, *Phys. Lett. B* **805** (2020) 135419, arXiv:1910.14407 [nucl-ex].
- [43] ALICE Collaboration, S. Acharya *et al.*, “Study of the Λ – Λ interaction with femtoscopy correlations in pp and p–Pb collisions at the LHC”, *Phys. Lett. B* **797** (2019) 134822, arXiv:1905.07209 [nucl-ex].
- [44] ALICE Collaboration, S. Acharya *et al.*, “First Observation of an Attractive Interaction between a Proton and a Cascade Baryon”, *Phys. Rev. Lett.* **123** (2019) 112002, arXiv:1904.12198 [nucl-ex].
- [45] ALICE Collaboration, S. Acharya *et al.*, “Unveiling the strong interaction among hadrons at the LHC”, *Nature* **588** (2020) 232–238, arXiv:2005.11495 [nucl-ex].
- [46] ALICE Collaboration, S. Acharya *et al.*, “Experimental evidence for an attractive p – ϕ interaction”, *Phys. Rev. Lett.* **127** (2021) 172301, arXiv:2105.05578 [nucl-ex].
- [47] ALICE Collaboration, S. Acharya *et al.*, “Investigating the role of strangeness in baryon–antibaryon annihilation at the LHC”, *Phys. Lett. B* **829** (2022) 137060, arXiv:2105.05190 [nucl-ex].
- [48] A. Hosaka, T. Hyodo, K. Sudoh, Y. Yamaguchi, and S. Yasui, “Heavy Hadrons in Nuclear Matter”, *Prog. Part. Nucl. Phys.* **96** (2017) 88–153, arXiv:1606.08685 [hep-ph].
- [49] H. Noumi, “Physics in J-PARC Hadron-Hall Extension”, *JPS Conf. Proc.* **13** (2017) 010017.
- [50] ALICE Collaboration, K. Aamodt *et al.*, “The ALICE experiment at the CERN LHC”, *J. Instrum.* **3** (2008) S08002.
- [51] ALICE Collaboration, B. B. Abelev *et al.*, “Performance of the ALICE Experiment at the CERN LHC”, *Int. J. Mod. Phys. A* **29** (2014) 1430044, arXiv:1402.4476 [nucl-ex].
- [52] ALICE Collaboration, K. Aamodt *et al.*, “Alignment of the ALICE Inner Tracking System with cosmic-ray tracks”, *JINST* **5** (2010) P03003, arXiv:1001.0502 [physics.ins-det].
- [53] J. Alme *et al.*, “The ALICE TPC, a large 3-dimensional tracking device with fast readout for ultra-high multiplicity events”, *Nucl. Instrum. Meth. A* **622** (2010) 316–367, arXiv:1001.1950 [physics.ins-det].
- [54] A. Akindinov *et al.*, “Performance of the ALICE Time-Of-Flight detector at the LHC”, *Eur. Phys. J. Plus* **128** (2013) 44.
- [55] ALICE Collaboration, E. Abbas *et al.*, “Performance of the ALICE VZERO system”, *JINST* **8** (2013) P10016, arXiv:1306.3130 [nucl-ex].
- [56] T. Sjöstrand, S. Mrenna, and P. Z. Skands, “PYTHIA 6.4 Physics and Manual”, *JHEP* **05** (2006) 026, arXiv:hep-ph/0603175.

- [57] T. Sjöstrand, S. Ask, J. R. Christiansen, R. Corke, N. Desai, P. Ilten, S. Mrenna, S. Prestel, C. O. Rasmussen, and P. Z. Skands, “An introduction to PYTHIA 8.2”, *Comput. Phys. Commun.* **191** (2015) 159–177, arXiv:1410.3012 [hep-ph].
- [58] P. Skands, S. Carrazza, and J. Rojo, “Tuning PYTHIA 8.1: the Monash 2013 Tune”, *Eur. Phys. J. C* **74** (2014) 3024, arXiv:1404.5630 [hep-ph].
- [59] R. Brun, F. Bruyant, M. Maire, A. C. McPherson, and P. Zancarini, *GEANT 3: user’s guide Geant 3.10, Geant 3.11; rev. version.* CERN, Geneva, 1987.
- [60] **Particle Data Group** Collaboration, P. A. Zyla *et al.*, “Review of Particle Physics”, *PTEP* **2020** (2020) 083C01.
- [61] T. Chen and C. Guestrin, “XGBoost: A scalable tree boosting system”, in *Proceedings of the 22nd ACM SIGKDD International Conference on Knowledge Discovery and Data Mining.* arXiv:1603.02754 [cs.LG].
- [62] L. Barioglio, F. Catalano, M. Concas, P. Fecchio, F. Grosa, F. Mazzaschi, and M. Puccio, “hipe4ml/hipe4ml”, July, 2021. <https://doi.org/10.5281/zenodo.5070132>.
- [63] **ALICE** Collaboration, S. Acharya *et al.*, “Measurement of beauty and charm production in pp collisions at $\sqrt{s} = 5.02$ TeV via non-prompt and prompt D mesons”, *JHEP* **05** (2021) 220, arXiv:2102.13601 [nucl-ex].
- [64] **ALICE** Collaboration, S. Acharya *et al.*, “Measurement of D^0 , D^+ , D^{*+} and D_s^+ production in pp collisions at $\sqrt{s} = 5.02$ TeV with ALICE”, *Eur. Phys. J. C* **79** (2019) 388, arXiv:1901.07979 [nucl-ex].
- [65] M. A. Lisa, S. Pratt, R. Soltz, and U. Wiedemann, “Femtoscopy in relativistic heavy ion collisions”, *Ann. Rev. Nucl. Part. Sci.* **55** (2005) 357–402, arXiv:nucl-ex/0505014.
- [66] **ALICE** Collaboration, S. Acharya *et al.*, “Search for a common baryon source in high-multiplicity pp collisions at the LHC”, *Phys. Lett. B* **811** (2020) 135849, arXiv:2004.08018 [nucl-ex].
- [67] I. G. Bearden *et al.*, “Space-time evolution of the hadronic source in peripheral to central Pb + Pb collisions”, *Eur. Phys. J. C* **18** (2000) 317–325.
- [68] A. Kisiel, M. Gałażyn, and P. Bożek, “Pion, kaon, and proton femtoscopy in Pb–Pb collisions at $\sqrt{s_{NN}}=2.76$ TeV modeled in (3+1)D hydrodynamics”, *Phys. Rev. C* **90** (2014) 064914, arXiv:1409.4571 [nucl-th].
- [69] V. M. Shapoval, P. Braun-Munzinger, I. A. Karpenko, and Y. M. Sinyukov, “Femtoscopy correlations of kaons in Pb+Pb collisions at LHC within hydrokinetic model”, *Nucl. Phys. A* **929** (2014) 1–8, arXiv:1404.4501 [hep-ph].
- [70] **CMS** Collaboration, A. M. Sirunyan *et al.*, “Studies of charm and beauty hadron long-range correlations in pp and pPb collisions at LHC energies”, *Phys. Lett. B* **813** (2021) 136036, arXiv:2009.07065 [hep-ex].
- [71] D. L. Mihaylov, V. Mantovani Sarti, O. W. Arnold, L. Fabbietti, B. Hohlweger, and A. M. Mathis, “A femtoscopic Correlation Analysis Tool using the Schrödinger equation (CATS)”, *Eur. Phys. J. C* **78** (2018) 394, arXiv:1802.08481 [hep-ph].
- [72] A. Kisiel, H. Zbroszczyk, and M. Szymański, “Extracting baryon-antibaryon strong interaction potentials from p $\bar{\Lambda}$ femtoscopic correlation functions”, *Phys. Rev. C* **89** (2014) 054916, arXiv:1403.0433 [nucl-th].

- [73] R. Lednicky, V. Lyuboshitz, and V. Lyuboshitz, “Final-state interactions in multichannel quantum systems and pair correlations of nonidentical and identical particles at low relative velocities”, *Physics of Atomic Nuclei* **61** (11, 1998) 2050–2063.
- [74] Y. Kamiya, T. Hyodo, K. Morita, A. Ohnishi, and W. Weise, “ $K^- p$ Correlation Function from High-Energy Nuclear Collisions and Chiral SU(3) Dynamics”, *Phys. Rev. Lett.* **124** (2020) 132501, arXiv:1911.01041 [nucl-th].
- [75] ALICE Collaboration, S. Acharya *et al.*, “Future high-energy pp programme with ALICE”, Tech. Rep. ALICE-PUBLIC-2020-005, 2020. <https://cds.cern.ch/record/2724925>.

A The ALICE Collaboration

S. Acharya¹⁴⁴, D. Adamová⁹⁷, A. Adler⁷⁵, J. Adolfsson⁸², G. Aglieri Rinella³⁴, M. Agnello³⁰, N. Agrawal⁵⁴, Z. Ahammed¹⁴⁴, S. Ahmad¹⁶, S.U. Ahn⁷⁷, I. Ahuja³⁸, Z. Akbar⁵¹, A. Akindinov⁹⁴, M. Al-Turany¹⁰⁹, S.N. Alam¹⁶, D. Aleksandrov⁹⁰, B. Alessandro⁵⁹, H.M. Alfanda⁷, R. Alfaro Molina⁷², B. Ali¹⁶, Y. Ali¹⁴, A. Alici²⁵, N. Alizadehvandchali¹²⁷, A. Alkin³⁴, J. Alme²¹, G. Alocco⁵⁵, T. Alt⁶⁹, I. Altsybeev¹¹⁵, M.N. Anaam⁷, C. Andrei⁴⁸, D. Andreou⁹², A. Andronic¹⁴⁷, V. Anguelov¹⁰⁶, F. Antinori⁵⁷, P. Antonioli⁵⁴, C. Anuj¹⁶, N. Apadula⁸¹, L. Aphecetche¹¹⁷, H. Appelshäuser⁶⁹, S. Arcelli²⁵, R. Arnaldi⁵⁹, I.C. Arsene²⁰, M. Arslandok¹⁴⁹, A. Augustinus³⁴, R. Averbeck¹⁰⁹, S. Aziz⁷⁹, M.D. Azmi¹⁶, A. Badalà⁵⁶, Y.W. Baek⁴¹, X. Bai^{131,109}, R. Bailhache⁶⁹, Y. Bailung⁵⁰, R. Bala¹⁰³, A. Balbino³⁰, A. Baldisseri¹⁴¹, B. Balis², D. Banerjee⁴, Z. Banoo¹⁰³, R. Barbera²⁶, L. Barioglio¹⁰⁷, M. Barlou⁸⁶, G.G. Barnaföldi¹⁴⁸, L.S. Barnby⁹⁶, V. Barret¹³⁸, C. Bartels¹³⁰, K. Barth³⁴, E. Bartsch⁶⁹, F. Baruffaldi²⁷, N. Bastid¹³⁸, S. Basu⁸², G. Batigne¹¹⁷, D. Battistini¹⁰⁷, B. Batyunya⁷⁶, D. Bauri⁴⁹, J.L. Bazo Alba¹¹⁴, I.G. Bearden⁹¹, C. Beattie¹⁴⁹, P. Becht¹⁰⁹, I. Belikov¹⁴⁰, A.D.C. Bell Hechavarria¹⁴⁷, F. Bellini²⁵, R. Bellwied¹²⁷, S. Belokurova¹¹⁵, V. Belyaev⁹⁵, G. Bencedi^{148,70}, S. Beole²⁴, A. Bercuci⁴⁸, Y. Berdnikov¹⁰⁰, A. Berdnikova¹⁰⁶, L. Bergmann¹⁰⁶, M.G. Besoiu⁶⁸, L. Betev³⁴, P.P. Bhaduri¹⁴⁴, A. Bhasin¹⁰³, I.R. Bhat¹⁰³, M.A. Bhat⁴, B. Bhattacharjee⁴², P. Bhattacharya²², L. Bianchi²⁴, N. Bianchi⁵², J. Bielčák³⁷, J. Bielčíková⁹⁷, J. Biernat¹²⁰, A. Bilandzic¹⁰⁷, G. Biro¹⁴⁸, S. Biswas⁴, J.T. Blair¹²¹, D. Blau^{90,83}, M.B. Blidaru¹⁰⁹, C. Blume⁶⁹, G. Boca^{28,58}, F. Bock⁹⁸, A. Bogdanov⁹⁵, S. Boi²², J. Bok⁶¹, L. Boldizsár¹⁴⁸, A. Bolozdynya⁹⁵, M. Bombara³⁸, P.M. Bond³⁴, G. Bonomi^{143,58}, H. Borel¹⁴¹, A. Borissov⁸³, H. Bossi¹⁴⁹, E. Botta²⁴, L. Bratrud⁶⁹, P. Braun-Munzinger¹⁰⁹, M. Bregant¹²³, M. Broz³⁷, G.E. Bruno^{108,33}, M.D. Buckland^{23,130}, D. Budnikov¹¹¹, H. Buesching⁶⁹, S. Bufalino³⁰, O. Bugnon¹¹⁷, P. Buhler¹¹⁶, Z. Buthelezi^{73,134}, J.B. Butt¹⁴, A. Bylinkin¹²⁹, S.A. Bysiak¹²⁰, M. Cai^{27,7}, H. Caines¹⁴⁹, A. Caliva¹⁰⁹, E. Calvo Villar¹¹⁴, J.M.M. Camacho¹²², R.S. Camacho⁴⁵, P. Camerini²³, F.D.M. Canedo¹²³, M. Carabas¹³⁷, F. Carnesecchi^{34,25}, R. Caron^{139,141}, J. Castillo Castellanos¹⁴¹, E.A.R. Casula²², F. Catalano³⁰, C. Ceballos Sanchez⁷⁶, I. Chakaberia⁸¹, P. Chakraborty⁴⁹, S. Chandra¹⁴⁴, S. Chapeland³⁴, M. Chartier¹³⁰, S. Chattopadhyay¹⁴⁴, S. Chattopadhyay¹¹², T.G. Chavez⁴⁵, T. Cheng⁷, C. Cheshkov¹³⁹, B. Cheynis¹³⁹, V. Chibante Barroso³⁴, D.D. Chinellato¹²⁴, S. Cho⁶¹, P. Chochula³⁴, P. Christakoglou⁹², C.H. Christensen⁹¹, P. Christiansen⁸², T. Chujo¹³⁶, C. Cicalo⁵⁵, L. Cifarelli²⁵, F. Cindolo⁵⁴, M.R. Ciupek¹⁰⁹, G. Clai^{54,ii}, J. Cleymans^{126,i}, F. Colamaria⁵³, J.S. Colburn¹¹³, D. Colella^{53,108,33}, A. Collu⁸¹, M. Colocci^{25,34}, M. Concas^{59,iii}, G. Conesa Balbastre⁸⁰, Z. Conesa del Valle⁷⁹, G. Contin²³, J.G. Contreras³⁷, M.L. Coquet¹⁴¹, T.M. Cormier⁹⁸, P. Cortese³¹, M.R. Cosentino¹²⁵, F. Costa³⁴, S. Costanza^{28,58}, P. Crochet¹³⁸, R. Cruz-Torres⁸¹, E. Cuautle⁷⁰, P. Cui⁷, L. Cunqueiro⁹⁸, A. Dainese⁵⁷, M.C. Danisch¹⁰⁶, A. Danu⁶⁸, P. Das⁸⁸, P. Das⁴, S. Das⁴, S. Dash⁴⁹, A. De Caro²⁹, G. de Cataldo⁵³, L. De Cilladi²⁴, J. de Cuveland³⁹, A. De Falco²², D. De Gruttola²⁹, N. De Marco⁵⁹, C. De Martin²³, S. De Pasquale²⁹, S. Deb⁵⁰, H.F. Degenhardt¹²³, K.R. Deja¹⁴⁵, R. Del Grande¹⁰⁷, L. Dello Stritto²⁹, W. Deng⁷, P. Dhankher¹⁹, D. Di Bari³³, A. Di Mauro³⁴, R.A. Diaz⁸, T. Dietel¹²⁶, Y. Ding^{139,7}, R. Divià³⁴, D.U. Dixit¹⁹, Ø. Djuvsland²¹, U. Dmitrieva⁶⁴, J. Do⁶¹, A. Dobrin⁶⁸, B. Dönigus⁶⁹, A.K. Dubey¹⁴⁴, A. Dubla^{109,92}, S. Dudi¹⁰², P. Dupieux¹³⁸, M. Durkac¹¹⁹, N. Dzalaiova¹³, T.M. Eder¹⁴⁷, R.J. Ehlers⁹⁸, V.N. Eikeland²¹, F. Eisenhut⁶⁹, D. Elia⁵³, B. Erazmus¹¹⁷, F. Ercolessi²⁵, F. Erhardt¹⁰¹, A. Erokhin¹¹⁵, M.R. Ersdal²¹, B. Espagnon⁷⁹, G. Eulisse³⁴, D. Evans¹¹³, S. Evdokimov⁹³, L. Fabbietti¹⁰⁷, M. Faggin²⁷, J. Faivre⁸⁰, F. Fan⁷, W. Fan⁸¹, A. Fantoni⁵², M. Fasel⁹⁸, P. Fedichio³⁰, A. Feliciello⁵⁹, G. Feofilov¹¹⁵, A. Fernández Téllez⁴⁵, A. Ferrero¹⁴¹, A. Ferretti²⁴, V.J.G. Feuillard¹⁰⁶, J. Figiel¹²⁰, V. Filova³⁷, D. Finogeev⁶⁴, F.M. Fionda⁵⁵, G. Fiorenza³⁴, F. Flor¹²⁷, A.N. Flores¹²¹, S. Foertsch⁷³, S. Fokin⁹⁰, E. Fragiaco⁶⁰, E. Frajna¹⁴⁸, A. Francisco¹³⁸, U. Fuchs³⁴, N. Funicello²⁹, C. Furget⁸⁰, A. Furs⁶⁴, J.J. Gaardhøje⁹¹, M. Gagliardi²⁴, A.M. Gago¹¹⁴, A. Gal¹⁴⁰, C.D. Galvan¹²², P. Ganoti⁸⁶, C. Garabatos¹⁰⁹, J.R.A. Garcia⁴⁵, E. Garcia-Solis¹⁰, K. Garg¹¹⁷, C. Gargiulo³⁴, A. Garibli⁸⁹, K. Garner¹⁴⁷, P. Gasik¹⁰⁹, E.F. Gauger¹²¹, A. Gautam¹²⁹, M.B. Gay Ducati⁷¹, M. Germain¹¹⁷, S.K. Ghosh⁴, M. Giacalone²⁵, P. Gianotti⁵², P. Giubellino^{109,59}, P. Giubilato²⁷, A.M.C. Glaenger¹⁴¹, P. Glässel¹⁰⁶, E. Glimos¹³³, D.J.Q. Goh⁸⁴, V. Gonzalez¹⁴⁶, L.H. González-Trueba⁷², S. Gorbunov³⁹, M. Gorgon², L. Görlich¹²⁰, S. Gotovac³⁵, V. Grabski⁷², L.K. Graczykowski¹⁴⁵, L. Greiner⁸¹, A. Grelli⁶³, C. Grigoras³⁴, V. Grigoriev⁹⁵, S. Grigoryan^{76,1}, F. Grosa^{34,59}, J.F. Grosse-Oetringhaus³⁴, R. Grosso¹⁰⁹, D. Grund³⁷, G.G. Guardianio¹²⁴, R. Guernane⁸⁰, M. Guilbaud¹¹⁷, K. Gulbrandsen⁹¹, T. Gunji¹³⁵, W. Guo⁷, A. Gupta¹⁰³, R. Gupta¹⁰³, S.P. Guzman⁴⁵, L. Gyulai¹⁴⁸, M.K. Habib¹⁰⁹, C. Hadjidakis⁷⁹, J. Haidenbauer⁶², H. Hamagaki⁸⁴, M. Hamid⁷, R. Hannigan¹²¹, M.R. Haque¹⁴⁵, A. Harlanderova¹⁰⁹, J.W. Harris¹⁴⁹, A. Harton¹⁰, J.A. Hasenbichler³⁴, H. Hassan⁹⁸, D. Hatzifotiadou⁵⁴, P. Hauer⁴³, L.B. Havener¹⁴⁹, S.T. Heckel¹⁰⁷, E. Hellbär¹⁰⁹, H. Helstrup³⁶, T. Herman³⁷, G. Herrera Corral⁹, F. Herrmann¹⁴⁷, K.F. Hetland³⁶, B. Heybeck⁶⁹, H. Hillemanns³⁴, C. Hills¹³⁰, B. Hippolyte¹⁴⁰, B. Hofman⁶³, B. Hohlweger⁹², J. Honermann¹⁴⁷, G.H. Hong¹⁵⁰, D. Horak³⁷, S. Hornung¹⁰⁹,

A. Horzyk², R. Hosokawa¹⁵, Y. Hou⁷, P. Hristov³⁴, C. Hughes¹³³, P. Huhn⁶⁹, L.M. Huhta¹²⁸, C.V. Hulse⁷⁹,
 T.J. Humanic⁹⁹, H. Hushnud¹¹², L.A. Husova¹⁴⁷, A. Hutson¹²⁷, T. Hyodo¹¹⁰, J.P. Iddon^{34,130}, R. Ilkaev¹¹¹,
 H. Ilyas¹⁴, M. Inaba¹³⁶, G.M. Innocenti³⁴, M. Ippolitov⁹⁰, A. Isakov⁹⁷, T. Isidori¹²⁹, M.S. Islam¹¹²,
 M. Ivanov¹⁰⁹, V. Ivanov¹⁰⁰, V. Izucheev⁹³, M. Jablonski², B. Jacak⁸¹, N. Jacazio³⁴, P.M. Jacobs⁸¹,
 S. Jadlovská¹¹⁹, J. Jádlovský¹¹⁹, S. Jaelani⁶³, C. Jahnke^{124,123}, M.J. Jakubowska¹⁴⁵, A. Jalostra¹⁰³,
 M.A. Janik¹⁴⁵, T. Janson⁷⁵, M. Jercic¹⁰¹, O. Jevons¹¹³, A.A.P. Jimenez⁷⁰, F. Jonas^{98,147}, P.G. Jones¹¹³,
 J.M. Jowett^{34,109}, J. Jung⁶⁹, M. Jung⁶⁹, A. Junique³⁴, A. Jusko¹¹³, M.J. Kabus¹⁴⁵, J. Kaewjai¹¹⁸,
 P. Kalinák⁶⁵, A.S. Kalteyer¹⁰⁹, A. Kalweit³⁴, Y. Kamiya¹¹⁰, V. Kaplin⁹⁵, A. Karasu Uysal⁷⁸, D. Karatovic¹⁰¹,
 O. Karavichev⁶⁴, T. Karavicheva⁶⁴, P. Karczmarczyk¹⁴⁵, E. Karpechev⁶⁴, V. Kashyap⁸⁸, A. Kazantsev⁹⁰,
 U. Kebschull⁷⁵, R. Keidel⁴⁷, D.L.D. Keijdener⁶³, M. Keil³⁴, B. Ketzer⁴³, A.M. Khan⁷, S. Khan¹⁶,
 A. Khanzadeev¹⁰⁰, Y. Kharlov^{93,83}, A. Khatun¹⁶, A. Khuntia¹²⁰, B. Kileng³⁶, B. Kim^{17,61}, C. Kim¹⁷,
 D.J. Kim¹²⁸, E.J. Kim⁷⁴, J. Kim¹⁵⁰, J.S. Kim⁴¹, J. Kim¹⁰⁶, J. Kim⁷⁴, M. Kim¹⁰⁶, S. Kim¹⁸, T. Kim¹⁵⁰,
 S. Kirsch⁶⁹, I. Kisel³⁹, S. Kiselev⁹⁴, A. Kisiel¹⁴⁵, J.P. Kitowski², J.L. Klay⁶, J. Klein³⁴, S. Klein⁸¹,
 C. Klein-Bösing¹⁴⁷, M. Kleiner⁶⁹, T. Klemenz¹⁰⁷, A. Kluge³⁴, A.G. Knospe¹²⁷, C. Kobdaj¹¹⁸, T. Kollegger¹⁰⁹,
 A. Kondratyev⁷⁶, N. Kondratyeva⁹⁵, E. Kondratyuk⁹³, J. König⁶⁹, S.A. Königstorfer¹⁰⁷, P.J. Konopka³⁴,
 G. Kornakov¹⁴⁵, S.D. Koryciak², A. Kotliarov⁹⁷, O. Kovalenko⁸⁷, V. Kovalenko¹¹⁵, M. Kowalski¹²⁰,
 I. Králik⁶⁵, A. Kravčáková³⁸, L. Kreis¹⁰⁹, M. Krivda^{113,65}, F. Krizek⁹⁷, K. Krizkova Gajdosova³⁷,
 M. Kroesen¹⁰⁶, M. Krüger⁶⁹, D.M. Krupova³⁷, E. Kryshen¹⁰⁰, M. Krzewicki³⁹, V. Kučera³⁴, C. Kuhn¹⁴⁰,
 P.G. Kuijer⁹², T. Kumaoka¹³⁶, D. Kumar¹⁴⁴, L. Kumar¹⁰², N. Kumar¹⁰², S. Kundu³⁴, P. Kurashvili⁸⁷,
 A. Kurepin⁶⁴, A.B. Kurepin⁶⁴, A. Kuryakin¹¹¹, S. Kushpil⁹⁷, J. Kvapil¹¹³, M.J. Kweon⁶¹, J.Y. Kwon⁶¹,
 Y. Kwon¹⁵⁰, S.L. La Pointe³⁹, P. La Rocca²⁶, Y.S. Lai⁸¹, A. Lakrathok¹¹⁸, M. Lamanna³⁴, R. Langoy¹³²,
 P. Larionov^{34,52}, E. Laudi³⁴, L. Lautner^{34,107}, R. Lavicka^{116,37}, T. Lazareva¹¹⁵, R. Lea^{143,23,58},
 J. Lehrbach³⁹, R.C. Lemmon⁹⁶, I. León Monzón¹²², M.M. Lesch¹⁰⁷, E.D. Lesser¹⁹, M. Lettrich^{34,107},
 P. Lévai¹⁴⁸, X. Li¹¹, X.L. Li⁷, J. Lien¹³², R. Lietava¹¹³, B. Lim¹⁷, S.H. Lim¹⁷, V. Lindenstruth³⁹,
 A. Lindner⁴⁸, C. Lippmann¹⁰⁹, A. Liu¹⁹, D.H. Liu⁷, J. Liu¹³⁰, I.M. Lofnes²¹, V. Loginov⁹⁵, C. Loizides⁹⁸,
 P. Loncar³⁵, J.A. Lopez¹⁰⁶, X. Lopez¹³⁸, E. López Torres⁸, J.R. Luhder¹⁴⁷, M. Lunardon²⁷, G. Luparello⁶⁰,
 Y.G. Ma⁴⁰, A. Maevskaya⁶⁴, M. Mager³⁴, T. Mahmoud⁴³, A. Maire¹⁴⁰, M. Malaev¹⁰⁰, N.M. Malik¹⁰³,
 Q.W. Malik²⁰, S.K. Malik¹⁰³, L. Malinina^{76,iv}, D. Mal'Kevich⁹⁴, D. Mallick⁸⁸, N. Mallick⁵⁰,
 G. Mandaglio^{32,56}, V. Manko⁹⁰, F. Manso¹³⁸, V. Manzari⁵³, Y. Mao⁷, G.V. Margagliotti²³, A. Margotti⁵⁴,
 A. Marín¹⁰⁹, C. Markert¹²¹, M. Marquard⁶⁹, N.A. Martin¹⁰⁶, P. Martinengo³⁴, J.L. Martinez¹²⁷,
 M.I. Martínez⁴⁵, G. Martínez García¹¹⁷, S. Masciocchi¹⁰⁹, M. Masera²⁴, A. Masoni⁵⁵, L. Massacrier⁷⁹,
 A. Mastroserio^{142,53}, A.M. Mathis¹⁰⁷, O. Matonoha⁸², P.F.T. Matuoka¹²³, A. Matyja¹²⁰, C. Mayer¹²⁰,
 A.L. Mazuecos³⁴, F. Mazzaschi²⁴, M. Mazzilli³⁴, J.E. Mdhului¹³⁴, A.F. Mechler⁶⁹, Y. Melikyan⁶⁴,
 A. Menchaca-Rocha⁷², E. Meninno^{116,29}, A.S. Menon¹²⁷, M. Meres¹³, S. Mhlanga^{126,73}, Y. Miake¹³⁶,
 L. Micheletti⁵⁹, L.C. Migliorin¹³⁹, D.L. Mihaylov¹⁰⁷, K. Mikhaylov^{76,94}, A.N. Mishra¹⁴⁸, D. Miśkowiec¹⁰⁹,
 A. Modak⁴, A.P. Mohanty⁶³, B. Mohanty⁸⁸, M. Mohisin Khan^{16,v}, M.A. Molander⁴⁴, Z. Moravcova⁹¹,
 C. Mordasini¹⁰⁷, D.A. Moreira De Godoy¹⁴⁷, I. Morozov⁶⁴, A. Morsch³⁴, T. Mrnjavac³⁴, V. Muccifora⁵²,
 E. Mudnic³⁵, D. Mühlheim¹⁴⁷, S. Muhuri¹⁴⁴, J.D. Mulligan⁸¹, A. Mulliri²², M.G. Munhoz¹²³, R.H. Munzer⁶⁹,
 H. Murakami¹³⁵, S. Murray¹²⁶, L. Musa³⁴, J. Musinsky⁶⁵, J.W. Myrcha¹⁴⁵, B. Naik¹³⁴, R. Nair⁸⁷,
 B.K. Nandi⁴⁹, R. Nania⁵⁴, E. Nappi⁵³, A.F. Nassirpour⁸², A. Nath¹⁰⁶, C. Natrass¹³³, A. Neagu²⁰,
 A. Negru¹³⁷, L. Nellen⁷⁰, S.V. Nesbo³⁶, G. Neskovic³⁹, D. Nesterov¹¹⁵, B.S. Nielsen⁹¹, E.G. Nielsen⁹¹,
 S. Nikolaev⁹⁰, S. Nikulin⁹⁰, V. Nikulin¹⁰⁰, F. Noferini⁵⁴, S. Noh¹², P. Nomokonov⁷⁶, J. Norman¹³⁰,
 N. Novitzky¹³⁶, P. Nowakowski¹⁴⁵, A. Nyanin⁹⁰, J. Nystrand²¹, M. Ogino⁸⁴, A. Ohlson⁸², A. Ohnishi¹⁵¹,
 V.A. Okorokov⁹⁵, J. Oleniacz¹⁴⁵, A.C. Oliveira Da Silva¹³³, M.H. Oliver¹⁴⁹, A. Onnerstad¹²⁸,
 C. Oppedisano⁵⁹, A. Ortiz Velasquez⁷⁰, T. Osako⁴⁶, A. Oskarsson⁸², J. Otwinowski¹²⁰, M. Oya⁴⁶,
 K. Oyama⁸⁴, Y. Pachmayer¹⁰⁶, S. Padhan⁴⁹, D. Pagano^{143,58}, G. Paic⁷⁰, A. Palasciano⁵³, S. Panebianco¹⁴¹,
 J. Park⁶¹, J.E. Parkkila¹²⁸, S.P. Pathak¹²⁷, R.N. Patra^{103,34}, B. Paul²², H. Pei⁷, T. Peitzmann⁶³, X. Peng⁷,
 L.G. Pereira⁷¹, H. Pereira Da Costa¹⁴¹, D. Peresunko^{90,83}, G.M. Perez⁸, S. Perrin¹⁴¹, Y. Pestov⁵,
 V. Petráček³⁷, V. Petrov¹¹⁵, M. Petrovici⁴⁸, R.P. Pezzi^{117,71}, S. Piano⁶⁰, M. Pikna¹³, P. Pillot¹¹⁷,
 O. Pinazza^{54,34}, L. Pinsky¹²⁷, C. Pinto²⁶, S. Pisano⁵², M. Płoskoń⁸¹, M. Planinic¹⁰¹, F. Pliquett⁶⁹,
 M.G. Poghosyan⁹⁸, B. Polichtchouk⁹³, S. Politano³⁰, N. Poljak¹⁰¹, A. Pop⁴⁸, S. Porteboeuf-Houssais¹³⁸,
 J. Porter⁸¹, V. Pozdniakov⁷⁶, S.K. Prasad⁴, R. Preghenella⁵⁴, F. Prino⁵⁹, C.A. Pruneau¹⁴⁶, I. Pshenichnov⁶⁴,
 M. Puccio³⁴, S. Qiu⁹², L. Quaglia²⁴, R.E. Quishpe¹²⁷, S. Ragoni¹¹³, A. Rakotozafindrabe¹⁴¹, L. Ramello³¹,
 F. Rami¹⁴⁰, S.A.R. Ramirez⁴⁵, T.A. Rancien⁸⁰, R. Raniwala¹⁰⁴, S. Raniwala¹⁰⁴, S.S. Räsänen⁴⁴, R. Rath⁵⁰,
 I. Ravasenga⁹², K.F. Read^{98,133}, A.R. Redelbach³⁹, K. Redlich^{87,vi}, A. Rehman²¹, P. Reichelt⁶⁹, F. Reidt³⁴,
 H.A. Reme-ness³⁶, Z. Rescakova³⁸, K. Reygers¹⁰⁶, A. Riabov¹⁰⁰, V. Riabov¹⁰⁰, T. Richert⁸², M. Richter²⁰,

W. Riegler³⁴, F. Riggi²⁶, C. Ristea⁶⁸, M. Rodríguez Cahuantzi⁴⁵, K. Røed²⁰, R. Rogalev⁹³, E. Rogochaya⁷⁶, T.S. Rogoschinski⁶⁹, D. Rohr³⁴, D. Röhrich²¹, P.F. Rojas⁴⁵, S. Rojas Torres³⁷, P.S. Rokita¹⁴⁵, F. Ronchetti⁵², A. Rosano^{32,56}, E.D. Rosas⁷⁰, A. Rossi⁵⁷, A. Roy⁵⁰, P. Roy¹¹², S. Roy⁴⁹, N. Rubini²⁵, O.V. Rueda⁸², D. Ruggiano¹⁴⁵, R. Rui²³, B. Rumyantsev⁷⁶, P.G. Russek², R. Russo⁹², A. Rustamov⁸⁹, E. Ryabinkin⁹⁰, Y. Ryabov¹⁰⁰, A. Rybicki¹²⁰, H. Rytönen¹²⁸, W. Rzeska¹⁴⁵, O.A.M. Saarimaki⁴⁴, R. Sadek¹¹⁷, S. Sadovsky⁹³, J. Saetre²¹, K. Šafařík³⁷, S.K. Saha¹⁴⁴, S. Saha⁸⁸, B. Sahoo⁴⁹, P. Sahoo⁴⁹, R. Sahoo⁵⁰, S. Sahoo⁶⁶, D. Sahu⁵⁰, P.K. Sahu⁶⁶, J. Saini¹⁴⁴, S. Sakai¹³⁶, M.P. Salvan¹⁰⁹, S. Sambyal¹⁰³, T.B. Saramela¹²³, D. Sarkar¹⁴⁶, N. Sarkar¹⁴⁴, P. Sarma⁴², V.M. Sarti¹⁰⁷, M.H.P. Sas¹⁴⁹, J. Schambach⁹⁸, H.S. Scheid⁶⁹, C. Schiaua⁴⁸, R. Schicker¹⁰⁶, A. Schmah¹⁰⁶, C. Schmidt¹⁰⁹, H.R. Schmidt¹⁰⁵, M.O. Schmidt^{34,106}, M. Schmidt¹⁰⁵, N.V. Schmidt^{98,69}, A.R. Schmier¹³³, R. Schotter¹⁴⁰, J. Schukraft³⁴, K. Schwarz¹⁰⁹, K. Schweda¹⁰⁹, G. Scioli²⁵, E. Scomparin⁵⁹, J.E. Seger¹⁵, Y. Sekiguchi¹³⁵, D. Sekihata¹³⁵, I. Selyuzhenkov^{109,95}, S. Senyukov¹⁴⁰, J.J. Seo⁶¹, D. Serebryakov⁶⁴, L. Šeršnyte¹⁰⁷, A. Sevcenco⁶⁸, T.J. Shaba⁷³, A. Shabanov⁶⁴, A. Shabetai¹¹⁷, R. Shahoyan³⁴, W. Shaikh¹¹², A. Shangaraev⁹³, A. Sharma¹⁰², D. Sharma⁴⁹, H. Sharma¹²⁰, M. Sharma¹⁰³, N. Sharma¹⁰², S. Sharma¹⁰³, U. Sharma¹⁰³, A. Shatat⁷⁹, O. Sheibani¹²⁷, K. Shigaki⁴⁶, M. Shimomura⁸⁵, S. Shirinkin⁹⁴, Q. Shou⁴⁰, Y. Sibiriyak⁹⁰, S. Siddhanta⁵⁵, T. Siemiarz⁸⁷, T.F. Silva¹²³, D. Silvermyr⁸², T. Simantathammakul¹¹⁸, G. Simonetti³⁴, B. Singh¹⁰⁷, R. Singh⁸⁸, R. Singh¹⁰³, R. Singh⁵⁰, V.K. Singh¹⁴⁴, V. Singhal¹⁴⁴, T. Sinha¹¹², B. Sitar¹³, M. Sitta³¹, T.B. Skaali²⁰, G. Skorodumovs¹⁰⁶, M. Slupecki⁴⁴, N. Smirnov¹⁴⁹, R.J.M. Snellings⁶³, C. Soncco¹¹⁴, J. Song¹²⁷, A. Songmoolnak¹¹⁸, F. Soramel²⁷, S. Sorensen¹³³, I. Sputowska¹²⁰, J. Stachel¹⁰⁶, I. Stan⁶⁸, P.J. Steffanic¹³³, S.F. Stiefelmaier¹⁰⁶, D. Stocco¹¹⁷, I. Storehaug²⁰, M.M. Storetvedt³⁶, P. Stratmann¹⁴⁷, S. Strazzi²⁵, C.P. Stylianidis⁹², A.A.P. Suaide¹²³, C. Suire⁷⁹, M. Sukhanov⁶⁴, M. Suljic³⁴, R. Sultanov⁹⁴, V. Sumberia¹⁰³, S. Sumowidagdo⁵¹, S. Swain⁶⁶, A. Szabo¹³, I. Szarka¹³, U. Tabassam¹⁴, S.F. Taghavi¹⁰⁷, G. Taillepie^{109,138}, J. Takahashi¹²⁴, G.J. Tambave²¹, S. Tang^{138,7}, Z. Tang¹³¹, J.D. Tapia Takaki^{129,vii}, N. Tapus¹³⁷, M.G. Tarzila⁴⁸, A. Tauro³⁴, G. Tejada Muñoz⁴⁵, A. Telesca³⁴, L. Terlizzi²⁴, C. Terrevoli¹²⁷, G. Tersimonov³, S. Thakur¹⁴⁴, D. Thomas¹²¹, R. Tieulent¹³⁹, A. Tikhonov⁶⁴, A.R. Timmins¹²⁷, M. Tkacik¹¹⁹, A. Toia⁶⁹, N. Topilskaya⁶⁴, M. Toppi⁵², F. Torres-Acosta¹⁹, T. Tork⁷⁹, A.G. Torres Ramos³³, A. Trifiro^{32,56}, A.S. Triolo³², S. Tripathy^{54,70}, T. Tripathy⁴⁹, S. Trogolo^{34,27}, V. Trubnikov³, W.H. Trzaska¹²⁸, T.P. Trzcinski¹⁴⁵, A. Tumkin¹¹¹, R. Turrisi⁵⁷, T.S. Tveter²⁰, K. Ullaland²¹, A. Uras¹³⁹, M. Urioni^{58,143}, G.L. Usai²², M. Vala³⁸, N. Valle²⁸, S. Vallerio⁵⁹, L.V.R. van Doremalen⁶³, M. van Leeuwen⁹², R.J.G. van Weelden⁹², P. Vande Vyvre³⁴, D. Varga¹⁴⁸, Z. Varga¹⁴⁸, M. Varga-Kofarago¹⁴⁸, M. Vasileiou⁸⁶, A. Vasiliev⁹⁰, O. Vázquez Doce^{52,107}, V. Vechernin¹¹⁵, A. Velure²¹, E. Vercellin²⁴, S. Vergara Limón⁴⁵, L. Vermunt⁶³, R. Vértesi¹⁴⁸, M. Verweij⁶³, L. Vickovic³⁵, Z. Vilakazi¹³⁴, O. Villalobos Baillie¹¹³, G. Vino⁵³, A. Vinogradov⁹⁰, T. Virgili²⁹, V. Vislavicius⁹¹, A. Vodopyanov⁷⁶, B. Volkel^{34,106}, M.A. Völkl¹⁰⁶, K. Voloshin⁹⁴, S.A. Voloshin¹⁴⁶, G. Volpe³³, B. von Haller³⁴, I. Vorobyev¹⁰⁷, N. Vozniuk⁶⁴, J. Vrláková³⁸, B. Wagner²¹, C. Wang⁴⁰, D. Wang⁴⁰, M. Weber¹¹⁶, A. Wegrzynek³⁴, S.C. Wenzel³⁴, J.P. Wessels¹⁴⁷, S.L. Weyhiller¹⁴⁹, J. Wiechula⁶⁹, J. Wikne²⁰, G. Wilk⁸⁷, J. Wilkinson¹⁰⁹, G.A. Willems¹⁴⁷, B. Windelband¹⁰⁶, M. Winn¹⁴¹, W.E. Witt¹³³, J.R. Wright¹²¹, W. Wu⁴⁰, Y. Wu¹³¹, R. Xu⁷, A.K. Yadav¹⁴⁴, S. Yalcin⁷⁸, Y. Yamaguchi⁴⁶, K. Yamakawa⁴⁶, S. Yang²¹, S. Yano⁴⁶, Z. Yin⁷, I.-K. Yoo¹⁷, J.H. Yoon⁶¹, S. Yuan²¹, A. Yuncu¹⁰⁶, V. Zaccolo²³, C. Zampolli³⁴, H.J.C. Zanoli⁶³, F. Zanone¹⁰⁶, N. Zardoshti³⁴, A. Zarochentsev¹¹⁵, P. Závada⁶⁷, N. Zaviyalov¹¹¹, M. Zhalov¹⁰⁰, B. Zhang⁷, S. Zhang⁴⁰, X. Zhang⁷, Y. Zhang¹³¹, V. Zherebchevskii¹¹⁵, Y. Zhi¹¹, N. Zhigareva⁹⁴, D. Zhou⁷, Y. Zhou⁹¹, J. Zhu^{109,7}, Y. Zhu⁷, G. Zinovjev^{3,i}, N. Zurlo^{143,58}

Affiliation notes

- ⁱ Deceased
- ⁱⁱ Also at: Italian National Agency for New Technologies, Energy and Sustainable Economic Development (ENEA), Bologna, Italy
- ⁱⁱⁱ Also at: Dipartimento DET del Politecnico di Torino, Turin, Italy
- ^{iv} Also at: M.V. Lomonosov Moscow State University, D.V. Skobeltsyn Institute of Nuclear Physics, Moscow, Russia
- ^v Also at: Department of Applied Physics, Aligarh Muslim University, Aligarh, India
- ^{vi} Also at: Institute of Theoretical Physics, University of Wrocław, Poland
- ^{vii} Also at: University of Kansas, Lawrence, Kansas, United States

Collaboration Institutes

- ¹ A.I. Alikhanyan National Science Laboratory (Yerevan Physics Institute) Foundation, Yerevan, Armenia

- ² AGH University of Science and Technology, Cracow, Poland
- ³ Bogolyubov Institute for Theoretical Physics, National Academy of Sciences of Ukraine, Kiev, Ukraine
- ⁴ Bose Institute, Department of Physics and Centre for Astroparticle Physics and Space Science (CAPSS), Kolkata, India
- ⁵ Budker Institute for Nuclear Physics, Novosibirsk, Russia
- ⁶ California Polytechnic State University, San Luis Obispo, California, United States
- ⁷ Central China Normal University, Wuhan, China
- ⁸ Centro de Aplicaciones Tecnológicas y Desarrollo Nuclear (CEADEN), Havana, Cuba
- ⁹ Centro de Investigación y de Estudios Avanzados (CINVESTAV), Mexico City and Mérida, Mexico
- ¹⁰ Chicago State University, Chicago, Illinois, United States
- ¹¹ China Institute of Atomic Energy, Beijing, China
- ¹² Chungbuk National University, Cheongju, Republic of Korea
- ¹³ Comenius University Bratislava, Faculty of Mathematics, Physics and Informatics, Bratislava, Slovakia
- ¹⁴ COMSATS University Islamabad, Islamabad, Pakistan
- ¹⁵ Creighton University, Omaha, Nebraska, United States
- ¹⁶ Department of Physics, Aligarh Muslim University, Aligarh, India
- ¹⁷ Department of Physics, Pusan National University, Pusan, Republic of Korea
- ¹⁸ Department of Physics, Sejong University, Seoul, Republic of Korea
- ¹⁹ Department of Physics, University of California, Berkeley, California, United States
- ²⁰ Department of Physics, University of Oslo, Oslo, Norway
- ²¹ Department of Physics and Technology, University of Bergen, Bergen, Norway
- ²² Dipartimento di Fisica dell'Università and Sezione INFN, Cagliari, Italy
- ²³ Dipartimento di Fisica dell'Università and Sezione INFN, Trieste, Italy
- ²⁴ Dipartimento di Fisica dell'Università and Sezione INFN, Turin, Italy
- ²⁵ Dipartimento di Fisica e Astronomia dell'Università and Sezione INFN, Bologna, Italy
- ²⁶ Dipartimento di Fisica e Astronomia dell'Università and Sezione INFN, Catania, Italy
- ²⁷ Dipartimento di Fisica e Astronomia dell'Università and Sezione INFN, Padova, Italy
- ²⁸ Dipartimento di Fisica e Nucleare e Teorica, Università di Pavia, Pavia, Italy
- ²⁹ Dipartimento di Fisica 'E.R. Caianiello' dell'Università and Gruppo Collegato INFN, Salerno, Italy
- ³⁰ Dipartimento DISAT del Politecnico and Sezione INFN, Turin, Italy
- ³¹ Dipartimento di Scienze e Innovazione Tecnologica dell'Università del Piemonte Orientale and INFN Sezione di Torino, Alessandria, Italy
- ³² Dipartimento di Scienze MIFT, Università di Messina, Messina, Italy
- ³³ Dipartimento Interateneo di Fisica 'M. Merlin' and Sezione INFN, Bari, Italy
- ³⁴ European Organization for Nuclear Research (CERN), Geneva, Switzerland
- ³⁵ Faculty of Electrical Engineering, Mechanical Engineering and Naval Architecture, University of Split, Split, Croatia
- ³⁶ Faculty of Engineering and Science, Western Norway University of Applied Sciences, Bergen, Norway
- ³⁷ Faculty of Nuclear Sciences and Physical Engineering, Czech Technical University in Prague, Prague, Czech Republic
- ³⁸ Faculty of Science, P.J. Šafárik University, Košice, Slovakia
- ³⁹ Frankfurt Institute for Advanced Studies, Johann Wolfgang Goethe-Universität Frankfurt, Frankfurt, Germany
- ⁴⁰ Fudan University, Shanghai, China
- ⁴¹ Gangneung-Wonju National University, Gangneung, Republic of Korea
- ⁴² Gauhati University, Department of Physics, Guwahati, India
- ⁴³ Helmholtz-Institut für Strahlen- und Kernphysik, Rheinische Friedrich-Wilhelms-Universität Bonn, Bonn, Germany
- ⁴⁴ Helsinki Institute of Physics (HIP), Helsinki, Finland
- ⁴⁵ High Energy Physics Group, Universidad Autónoma de Puebla, Puebla, Mexico
- ⁴⁶ Hiroshima University, Hiroshima, Japan
- ⁴⁷ Hochschule Worms, Zentrum für Technologietransfer und Telekommunikation (ZTT), Worms, Germany
- ⁴⁸ Horia Hulubei National Institute of Physics and Nuclear Engineering, Bucharest, Romania
- ⁴⁹ Indian Institute of Technology Bombay (IIT), Mumbai, India
- ⁵⁰ Indian Institute of Technology Indore, Indore, India
- ⁵¹ Indonesian Institute of Sciences, Jakarta, Indonesia

- 52 INFN, Laboratori Nazionali di Frascati, Frascati, Italy
- 53 INFN, Sezione di Bari, Bari, Italy
- 54 INFN, Sezione di Bologna, Bologna, Italy
- 55 INFN, Sezione di Cagliari, Cagliari, Italy
- 56 INFN, Sezione di Catania, Catania, Italy
- 57 INFN, Sezione di Padova, Padova, Italy
- 58 INFN, Sezione di Pavia, Pavia, Italy
- 59 INFN, Sezione di Torino, Turin, Italy
- 60 INFN, Sezione di Trieste, Trieste, Italy
- 61 Inha University, Incheon, Republic of Korea
- 62 Institute for Advanced Simulation, Forschungszentrum Jülich, Jülich, Germany
- 63 Institute for Gravitational and Subatomic Physics (GRASP), Utrecht University/Nikhef, Utrecht, Netherlands
- 64 Institute for Nuclear Research, Academy of Sciences, Moscow, Russia
- 65 Institute of Experimental Physics, Slovak Academy of Sciences, Košice, Slovakia
- 66 Institute of Physics, Homi Bhabha National Institute, Bhubaneswar, India
- 67 Institute of Physics of the Czech Academy of Sciences, Prague, Czech Republic
- 68 Institute of Space Science (ISS), Bucharest, Romania
- 69 Institut für Kernphysik, Johann Wolfgang Goethe-Universität Frankfurt, Frankfurt, Germany
- 70 Instituto de Ciencias Nucleares, Universidad Nacional Autónoma de México, Mexico City, Mexico
- 71 Instituto de Física, Universidade Federal do Rio Grande do Sul (UFRGS), Porto Alegre, Brazil
- 72 Instituto de Física, Universidad Nacional Autónoma de México, Mexico City, Mexico
- 73 iThemba LABS, National Research Foundation, Somerset West, South Africa
- 74 Jeonbuk National University, Jeonju, Republic of Korea
- 75 Johann-Wolfgang-Goethe Universität Frankfurt Institut für Informatik, Fachbereich Informatik und Mathematik, Frankfurt, Germany
- 76 Joint Institute for Nuclear Research (JINR), Dubna, Russia
- 77 Korea Institute of Science and Technology Information, Daejeon, Republic of Korea
- 78 KTO Karatay University, Konya, Turkey
- 79 Laboratoire de Physique des 2 Infinis, Irène Joliot-Curie, Orsay, France
- 80 Laboratoire de Physique Subatomique et de Cosmologie, Université Grenoble-Alpes, CNRS-IN2P3, Grenoble, France
- 81 Lawrence Berkeley National Laboratory, Berkeley, California, United States
- 82 Lund University Department of Physics, Division of Particle Physics, Lund, Sweden
- 83 Moscow Institute for Physics and Technology, Moscow, Russia
- 84 Nagasaki Institute of Applied Science, Nagasaki, Japan
- 85 Nara Women's University (NWU), Nara, Japan
- 86 National and Kapodistrian University of Athens, School of Science, Department of Physics, Athens, Greece
- 87 National Centre for Nuclear Research, Warsaw, Poland
- 88 National Institute of Science Education and Research, Homi Bhabha National Institute, Jatni, India
- 89 National Nuclear Research Center, Baku, Azerbaijan
- 90 National Research Centre Kurchatov Institute, Moscow, Russia
- 91 Niels Bohr Institute, University of Copenhagen, Copenhagen, Denmark
- 92 Nikhef, National institute for subatomic physics, Amsterdam, Netherlands
- 93 NRC Kurchatov Institute IHEP, Protvino, Russia
- 94 NRC «Kurchatov»Institute - ITEP, Moscow, Russia
- 95 NRNU Moscow Engineering Physics Institute, Moscow, Russia
- 96 Nuclear Physics Group, STFC Daresbury Laboratory, Daresbury, United Kingdom
- 97 Nuclear Physics Institute of the Czech Academy of Sciences, Řež u Prahy, Czech Republic
- 98 Oak Ridge National Laboratory, Oak Ridge, Tennessee, United States
- 99 Ohio State University, Columbus, Ohio, United States
- 100 Petersburg Nuclear Physics Institute, Gatchina, Russia
- 101 Physics department, Faculty of science, University of Zagreb, Zagreb, Croatia
- 102 Physics Department, Panjab University, Chandigarh, India
- 103 Physics Department, University of Jammu, Jammu, India

- 104 Physics Department, University of Rajasthan, Jaipur, India
- 105 Physikalisches Institut, Eberhard-Karls-Universität Tübingen, Tübingen, Germany
- 106 Physikalisches Institut, Ruprecht-Karls-Universität Heidelberg, Heidelberg, Germany
- 107 Physik Department, Technische Universität München, Munich, Germany
- 108 Politecnico di Bari and Sezione INFN, Bari, Italy
- 109 Research Division and ExtreMe Matter Institute EMMI, GSI Helmholtzzentrum für Schwerionenforschung GmbH, Darmstadt, Germany
- 110 RIKEN iTHEMS, Wako, Japan
- 111 Russian Federal Nuclear Center (VNIIEF), Sarov, Russia
- 112 Saha Institute of Nuclear Physics, Homi Bhabha National Institute, Kolkata, India
- 113 School of Physics and Astronomy, University of Birmingham, Birmingham, United Kingdom
- 114 Sección Física, Departamento de Ciencias, Pontificia Universidad Católica del Perú, Lima, Peru
- 115 St. Petersburg State University, St. Petersburg, Russia
- 116 Stefan Meyer Institut für Subatomare Physik (SMI), Vienna, Austria
- 117 SUBATECH, IMT Atlantique, Université de Nantes, CNRS-IN2P3, Nantes, France
- 118 Suranaree University of Technology, Nakhon Ratchasima, Thailand
- 119 Technical University of Košice, Košice, Slovakia
- 120 The Henryk Niewodniczanski Institute of Nuclear Physics, Polish Academy of Sciences, Cracow, Poland
- 121 The University of Texas at Austin, Austin, Texas, United States
- 122 Universidad Autónoma de Sinaloa, Culiacán, Mexico
- 123 Universidade de São Paulo (USP), São Paulo, Brazil
- 124 Universidade Estadual de Campinas (UNICAMP), Campinas, Brazil
- 125 Universidade Federal do ABC, Santo Andre, Brazil
- 126 University of Cape Town, Cape Town, South Africa
- 127 University of Houston, Houston, Texas, United States
- 128 University of Jyväskylä, Jyväskylä, Finland
- 129 University of Kansas, Lawrence, Kansas, United States
- 130 University of Liverpool, Liverpool, United Kingdom
- 131 University of Science and Technology of China, Hefei, China
- 132 University of South-Eastern Norway, Tonsberg, Norway
- 133 University of Tennessee, Knoxville, Tennessee, United States
- 134 University of the Witwatersrand, Johannesburg, South Africa
- 135 University of Tokyo, Tokyo, Japan
- 136 University of Tsukuba, Tsukuba, Japan
- 137 University Politehnica of Bucharest, Bucharest, Romania
- 138 Université Clermont Auvergne, CNRS/IN2P3, LPC, Clermont-Ferrand, France
- 139 Université de Lyon, CNRS/IN2P3, Institut de Physique des 2 Infinis de Lyon, Lyon, France
- 140 Université de Strasbourg, CNRS, IPHC UMR 7178, F-67000 Strasbourg, France, Strasbourg, France
- 141 Université Paris-Saclay Centre d'Etudes de Saclay (CEA), IRFU, Département de Physique Nucléaire (DPhN), Saclay, France
- 142 Università degli Studi di Foggia, Foggia, Italy
- 143 Università di Brescia, Brescia, Italy
- 144 Variable Energy Cyclotron Centre, Homi Bhabha National Institute, Kolkata, India
- 145 Warsaw University of Technology, Warsaw, Poland
- 146 Wayne State University, Detroit, Michigan, United States
- 147 Westfälische Wilhelms-Universität Münster, Institut für Kernphysik, Münster, Germany
- 148 Wigner Research Centre for Physics, Budapest, Hungary
- 149 Yale University, New Haven, Connecticut, United States
- 150 Yonsei University, Seoul, Republic of Korea
- 151 Yukawa Institute for Theoretical Physics, Kyoto University, Kyoto, Japan